Swiss J Geosci (2016) 109:83–102
DOI 10.1007/s00015-016-0208-5

The St. Gallen Fault Zone: a long-lived, multiphase structure in the North Alpine Foreland Basin revealed by 3D seismic data

Stefan Heuberger[1] · Philippe Roth[1] · Olivier Zingg[2] · Henry Naef[3] · Beat P. Meier[1]

Received: 28 August 2015 / Accepted: 15 January 2016 / Published online: 8 February 2016
© Swiss Geological Society 2016

Abstract The St. Gallen Fault Zone (SFZ) is a system of major NNE–SSW striking normal faults within the North Alpine Foreland Basin (NAFB), just west of the city of St. Gallen. It used to be only roughly known from 2D seismic data, locally displaying offsets of up to 300 m at the level of the Mesozoic strata. We present a detailed structural interpretation of a recently acquired 3D seismic dataset that reveals the occurrence of multiphase tectonic activity along the SFZ from at least the Late Paleozoic to the early Oligocene, and possibly even later. We can show that the SFZ roots in extensional basement structures that bound small Permo-Carboniferous grabens. Thickness changes in the younger sediments above these Paleozoic grabens indicate several phases of tectonic subsidence during the Triassic and the Jurassic. The Lower Cenozoic units in the northernmost part of the 3D seismic area are also offset by the SFZ. No offsets can be identified in the overlying, shallower part of the Cenozoic units. Most faults constituting the SFZ are favourably oriented in the present-day stress field (S_{Hmax} NNW–SSE) to be reactivated in strike-slip mode. The seismic events induced by testing operations at the geothermal exploration borehole "St. Gallen GT-1" (SG GT-1) in July 2013 revealed that, even though the seismicity of northeastern Switzerland is considered to be low and diffuse, parts of the SFZ have to be regarded as critically stressed. Combining the interpretation of geological and seismic data, we conclude that the SFZ represents a reactivated basement-rooted normal fault, which was active during several phases in Permo-Carboniferous and Mesozoic times and that is still active today in strike-slip mode.

Keywords Structural geology · Reflection seismic data · Mesozoic synsedimentary faulting · Permo-Carboniferous grabens · Neotectonics · Induced seismicity · Geothermal Power Plant Project St. Gallen

Zusammenfassung Die St. Gallen-Verwerfungszone (SFZ) ist ein System markanter, NNE–SSW streichender Abschiebungen im Nordalpinen Vorlandbecken. Sie liegt unmittelbar westlich der Stadt St. Gallen. Ihre Geometrie ist, basierend auf 2D-Seismik-Daten, ungefähr bekannt; sie versetzt die gesamte Mesozoische Schichtfolge um bis zu 300 m. Wir präsentieren eine strukturelle Auswertung eines neuen 3D-Seismikdatensatzes, die eine mehrphasige tektonische Aktivität entlang der SFZ seit mindestens dem Permo-Karbon bis ins frühe Oligozän oder vermutlich noch später aufzeigt. Demnach wurzelt die SFZ in extensionalen Grundgebirgsstrukturen, welche Rand-Verwerfungen von kleinen Permo-Karbon-Trögen entsprechen. Mächtigkeitsschwankungen in jüngeren Sedimenten oberhalb dieser Paläozoischen Tröge bezeugen mehrere Phasen tektonischer Subsidenz während der Trias und dem Jura. Ganz im Norden des 3D-Untersuchungsgebiets ist auch das untere Tertiär durch die SFZ versetzt. Im darüber liegenden restlichen Teil des Tertiärs sind keine Versätze kartierbar. Die meisten Verwerfungen der SFZ sind für eine Reaktivierung als Strike-Slip-Verwerfung im rezenten Spannungsfeld (S_{Hmax} NNW–SSE) günstig orientiert. Obwohl

Editorial handling: Communicated by S. Schmid.

✉ Stefan Heuberger
stefan.heuberger@alumni.ethz.ch

[1] Proseis AG, Schaffhauserstrasse 418, 8050 Zurich, Switzerland

[2] Geo-Energie-Suisse AG, Reitergasse 11, 8004 Zurich, Switzerland

[3] Geosfer AG, Teufenerstrasse 3, 9000 St. Gallen, Switzerland

die Seismizität in der Nordostschweiz als gering und diffus betrachtet wird, machen die durch die Test-Operationen in der Geothermie-Explorationsbohrung „St. Gallen GT-1“ (SG GT-1) im Juli 2013 induzierten Erdbeben deutlich, dass Teile der SFZ als kritisch gespannt zu betrachten sind. Die SFZ kann anhand unseres Datensatzes als eine im Grundgebirge angelegte, reaktivierte Abschiebung betrachtet werden, die während mehrerer Zeitabschnitte im Jungpaläozoikum und Mesozoikum aktiv war und es als Blattverschiebung heute noch ist.

1 Introduction

Major fault zones are only sparsely known in the North Alpine Foreland Basin (NAFB) of central and eastern Switzerland, especially fault zones that strike transverse to the basin's axis. A new 3D seismic dataset as well as seismicity induced by operations at the geothermal exploration borehole "St. Gallen GT-1" (SG GT-1) provide valuable data for the structural and kinematic analysis of the region. This study is based on a detailed interpretation of the 3D seismic dataset and intends to delineate the geometry and kinematics of the St. Gallen Fault Zone (SFZ) and to characterise its position in the regional tectonic context. The c. 20 km long SFZ was so far only known from offset seismic horizons at the level of the Mesozoic strata interpreted on 2D seismic lines between Lake Constance and St. Gallen (Fig. 1; Roth et al. 2010). Its seismogenic nature was not known at all.

On the basis of a 3D seismic interpretation, we derived a detailed structural model allowing us to integrate the seismic events of 2013, that occurred at the borehole SG GT-1, into the local kinematic setting. Furthermore, we discuss the problem of whether the SFZ can be traced from the Mesozoic sequence across the c. 2.5–3.5 km thick pile of laterally discontinuous Cenozoic Molasse units. Re-evaluation of existing 2D seismic interpretations to the north of the 3D seismic area allowed us to better constrain the relationship of the SFZ with a major NW–SE striking fault that is probably part of the Hegau-Lake Constance Graben system. The structural model also resulted in thickness maps, which illustrate several phases of synsedimentary faulting in Mesozoic times. Combining these maps with amplitude extractions from sub-Mesozoic intervals and with the reflection seismic interpretation, we can show where the SFZ faults originate in the basement and how they are related to Permo-Carboniferous (PC) grabens.

2 Geological setting

2.1 Overview

The study area is located in the eastern part of the NAFB of northeastern Switzerland, east of the Jura fold-and-thrust belt and hence outside of the detached part of the Molasse Basin. This location might be a reason why knowledge of its tectonic evolution is less constrained in comparison with the western part of the NAFB. Major tectonic structures in the area are the Hegau-Lake Constance Graben System (e.g. Carlé 1955) in the north, and the Baden–Irchel–Herdern Lineament (e.g. Nagra 2008) and the Alpine Front in the south (Fig. 1). Reflection seismic data were collected by the hydrocarbon industry and by Nagra (Nationale Genossenschaft für die Lagerung radioaktiver Abfälle) mainly between 1970 and 1996 across most of the NAFB (Sprecher and Müller 1986; Diebold et al. 1991; Naef et al. 1995; Birkhäuser et al. 2001; Nagra 2008; note that all Nagra reports cited in this article can be downloaded from the Nagra website). These data showed that the normal faults of the SFZ form a major NNE–SSW striking structure offsetting the entire Mesozoic sedimentary cover. The fault zone's topmost, Cenozoic extent remained widely unknown as it is difficult to trace in the Molasse units. Moreover, its potential surface (Quaternary) expression is obliterated by young glacial deposits. With its NNE–SSW strike, transverse to the foreland basin's SW–NE strike, the SFZ represents a rather unique, major structure in the central and eastern Swiss NAFB. Although previous authors (Roth et al. 2010) interpreted the northern termination of the SFZ to bend anti-clockwise towards a NW–SE strike, the relationship of the SFZ with the southeasternmost extensions of the NW–SE striking Hegau-Lake Constance Graben faults is unknown.

The NAFB is a peripheral foredeep that formed by flexural bending of the European lithosphere in response to crustal thickening in the Alpine orogen during the Cenozoic (e.g. Allen et al. 1986) and/or slab pull and rollback of the European mantle lithosphere (Schlunegger and Kissling 2015). It comprises Oligo-Miocene deposits that were categorised into four lithostratigraphic units (Matter et al. 1980; Homewood et al. 1986; Pfiffner 1986) from bottom to top: Lower Marine Molasse "Untere Meeresmolasse" (UMM), Lower Freshwater Molasse "Untere Süsswassermolasse" (USM), Upper Marine Molasse "Obere Meeresmolasse" (OMM) and Upper Freshwater Molasse "Obere Süsswassermolasse" (OSM). They represent two progradational and regressive megasequences recording the transition from the initial underfilled Flysch to the overfilled Molasse stage during the evolution of the NAFB

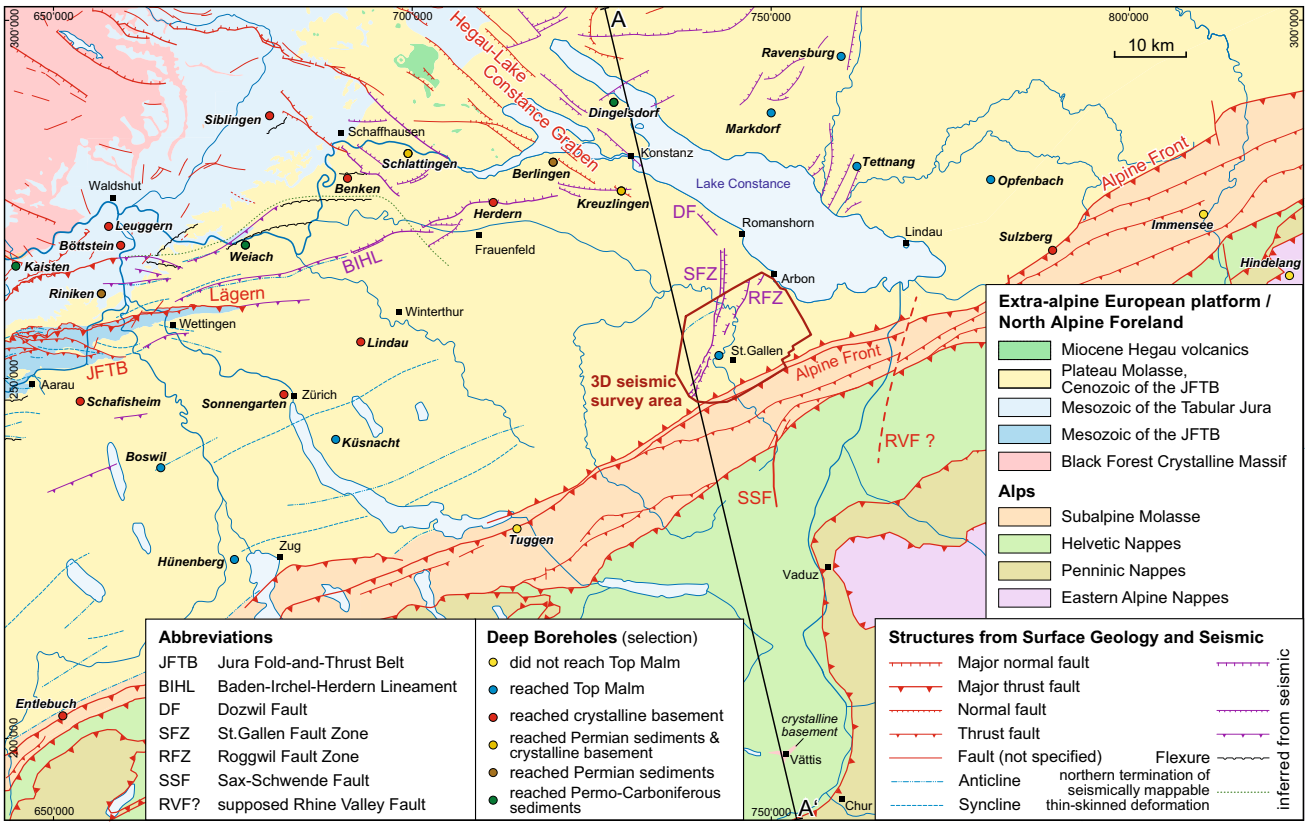


Fig. 1 Tectonic overview of northeastern Switzerland and adjacent areas modified from Swisstopo (2005), Pfiffner et al. (2010), Roth et al. (2010) and this study (within the 3D seismic survey area). The faults derived from 2D seismic data north of Lake Constance are modified from Volz (1957), Bachmann et al. 1982 and Reicherter et al. (2008). Cross-section AA′ is shown in Fig. 2. The indicated boreholes represent a subset of all existing deep boreholes

(Sinclair and Allen 1992). The Molasse is structurally subdivided into the flat-lying to inclined Plateau Molasse in the north and the folded and thrusted Subalpine Molasse in the south (e.g. Burkhard 1990). The Subalpine Molasse consists of imbricate wedges of Molasse sediments overthrusted by the Helvetic Nappes from the south (Figs. 1, 2). The backthrusted and thus inclined southernmost Plateau Molasse, together with the northernmost wedges of the Subalpine Molasse, form a triangle zone representing the most external Alpine tectonic structure in northeastern Switzerland (Fig. 2). The Cenozoic Molasse units discordantly overlie the primarily marine, slightly SSE dipping, Mesozoic sedimentary sequence represented by Triassic to Jurassic formations (Fig. 3). Cretaceous sediments are not present as they were either not deposited or were eroded before the deposition of the Molasse. Evidence for tectonic deformation during Mesozoic times is only sparse (e.g. Sommaruga 2011), for example in Upper Triassic to Middle Jurassic units (Birkhäuser et al. 2001; Marchant et al. 2005), or is indirectly inferred by sedimentological studies (e.g. Wetzel et al. 2003; Allenbach and Wetzel 2006). The base Mesozoic is represented by a gently SE dipping, post-Variscan unconformity (Sprecher and Müller 1986; Diebold et al. 1991). The basement is regionally segmented into mainly WSW–ENE trending PC grabens that formed by dextral transtension tectonics during the Late Paleozoic (e.g. Diebold et al. 1991; McCann et al. 2006).

2.2 Tectonic setting of the St. Gallen 3D seismic survey area

The St. Gallen 3D seismic survey area is located at the transition of the Plateau to the Subalpine Molasse representing the Alpine Front (Figs. 1, 2). Further north, there are no thrusts related to the Alpine deformation, rooting in the basement of the external massifs, as it is the case in the classical Jura fold-and-thrust belt. Towards the west, the closest surface expression of Alpine thrusting related to the detachment along the Triassic evaporites is the Lägern Anticline, marking the easternmost expression of the Jura fold-and-thrust belt (Burkhard 1990). East of the Lägern,

compressional faulting is only known from seismic data; the northern termination of the seismically mappable thin-skinned deformation is only poorly constrained (Naef et al. 1985; Naef et al. 1995; Müller et al. 2002; Madritsch 2015). This Alpine deformation front thus steps back in the area of Winterthur–Frauenfeld (Fig. 1) from the Jura front and its eastern extension to the southern edge of the Plateau Molasse (Burkhard 1990). Here, shortening took place above an assumed basal décollement, somewhere near the base Cenozoic, and led to the formation of a basal blind thrust overlain by a triangle zone (Pfiffner 1986; Müller et al. 1988; Pfiffner et al. 1997; Berge and Veal 2005; Fig. 2). Analysing deformed fossils and conglomerate pebbles, Breddin (1964) and Schrader (1988) inferred substantial internal deformation in the order of 20 % within the Plateau Molasse to the north of the triangle zone. This claimed shortening seems incompatible with the underlying stiff Upper Jurassic Malm formation that does not exhibit any folds or thrusts resolvable by reflection seismic data (Burkhard 1990). No major strike-slip faults, as documented in the western Molasse Basin, are known from surface geology or reflection seismic data in northeastern Switzerland (Roth et al. 2010).

The structural setting of the Mesozoic sequence and the underlying basement is poorly constrained in the St. Gallen area. The few known normal faults that strike parallel to the Alpine mountain range were formed or reactivated primarily in Oligocene times due to flexural bending of the European plate during Alpine convergence (e.g. Pfiffner 1986). Such normal faults, extending up to Upper Oligocene Molasse deposits, are documented by e.g. the Baden–Irchel–Herdern Lineament (Fig. 1; Nagra 2008) as well as by several faults east of Lake Constance in the better explored Bavarian Molasse (e.g. Bachmann et al. 1982; Rupf and Nitsch 2008). Leu (2008) compiled 2D seismic interpretations and tentatively mapped a NNE–SSW trending PC graben between St. Gallen and Lake Constance that appears to be related to the SFZ.

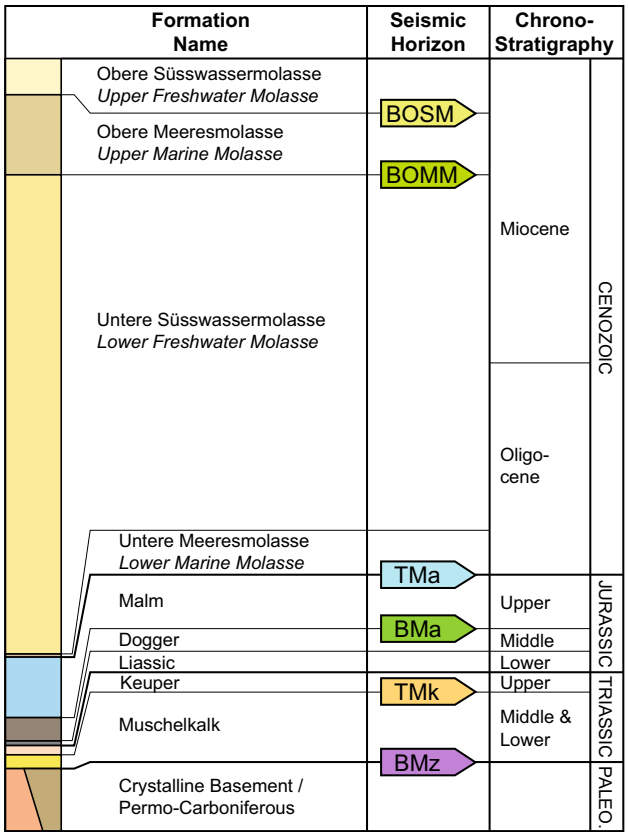


Fig. 3 Chronostratigraphy and formation names with seismic horizons. *BOSM* Base Upper Freshwater Molasse, *BOMM* Base Upper Marine Molasse, *TMa* Top Malm, *BMa* Base Malm, *TMk* Top Muschelkalk, *BMz* Base Mesozoic

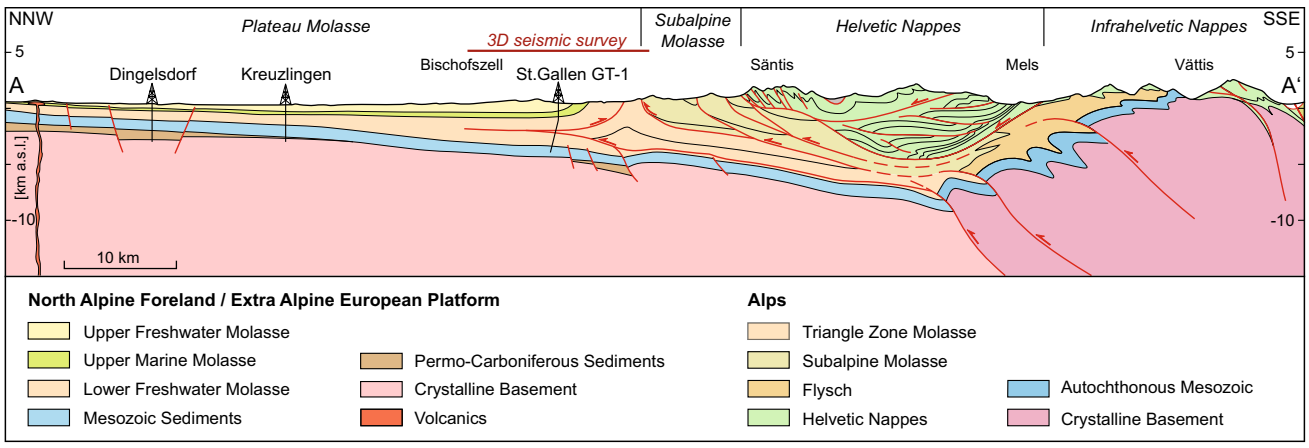


Fig. 2 Tectonic cross-section across northeastern Switzerland, modified from Swisstopo (2005). See section trace in Fig. 1. The 3D seismic survey is located in the transition area between the Plateau Molasse and the Subalpine Molasse, forming a triangle zone. Note that the borehole trajectory of St. Gallen GT-1 is projected over a distance of c. 4 km

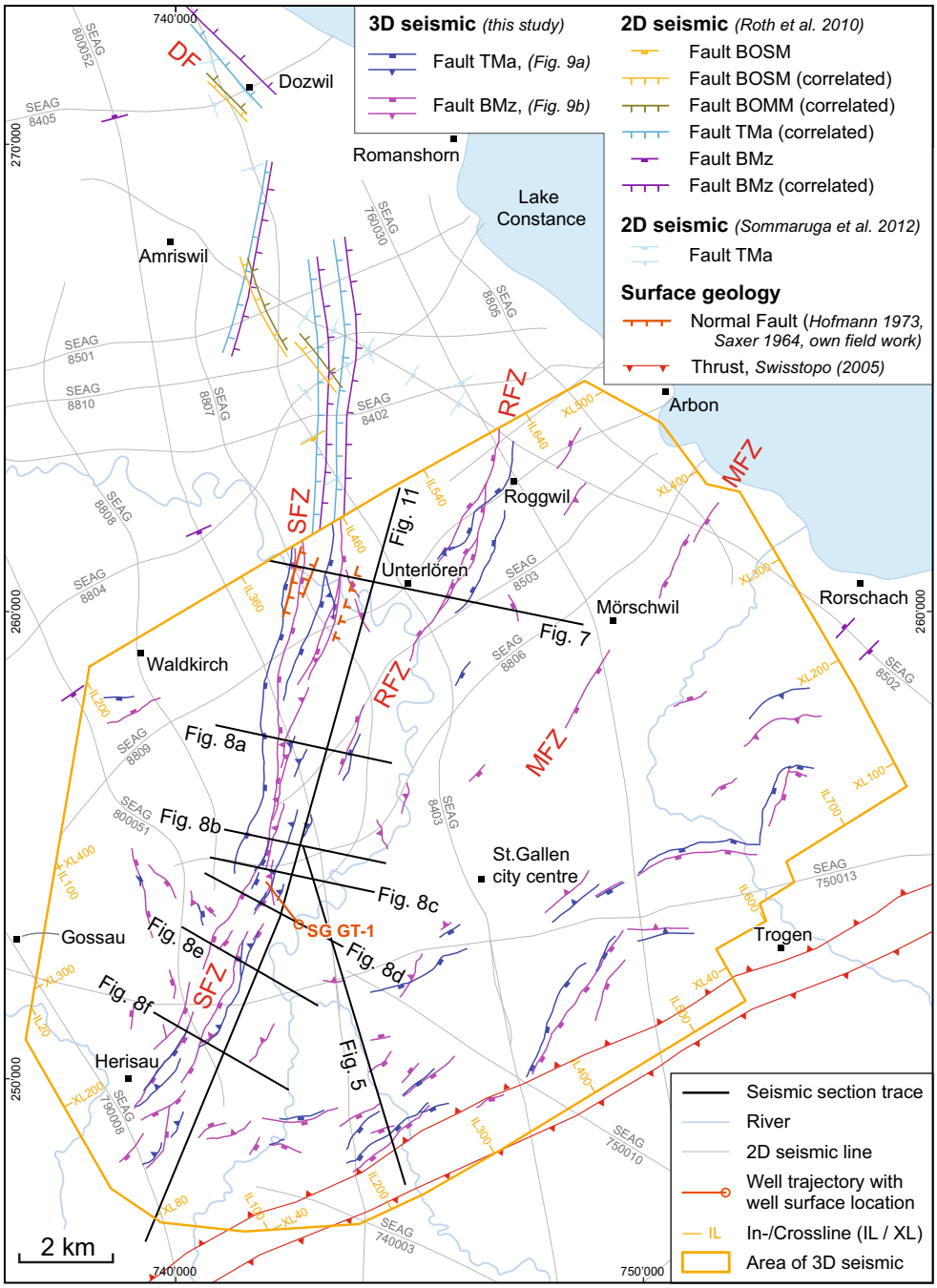


Fig. 4 Structural overview and location of cross-sections and of seismic data. Faults mapped from 2D seismic are not shown within the 3D seismic area. *DF* Dozwil Fault, *SFZ* St. Gallen Fault Zone, *RFZ* Roggwil Fault Zone, *MFZ* Mörschwil Fault Zone

3 Seismic survey and interpretation of horizons and faults

The St. Gallen 3D seismic data were collected during winter and spring 2009/2010 with a survey covering an area of about 270 km^2 (Fig. 4). Along 21 SW–NE striking source lines comprising more than 6300 locations, seismic waves were excited every 50 m primarily by vibroseis and accessorily by explosive sources (c. 250 locations). 11,400 receiver stations were placed every 50 m along 42 NW–SE oriented receiver lines. This results in a bin size of 25 by 25 m and in a nominal 40-fold coverage (the number of common subsurface mid points that fall into the same bin). A Prestack Time Migration (PSTM) with CRS (Common Reflection Surface) processing was used for the interpretation (for details on seismic nomenclature see e.g. Madritsch et al. 2013). To support the structural interpretation, a coherence volume (e.g. Marfurt et al. 1999) was computed from the 3D seismic data to highlight reflection discontinuities. Although seismic data were acquired in a

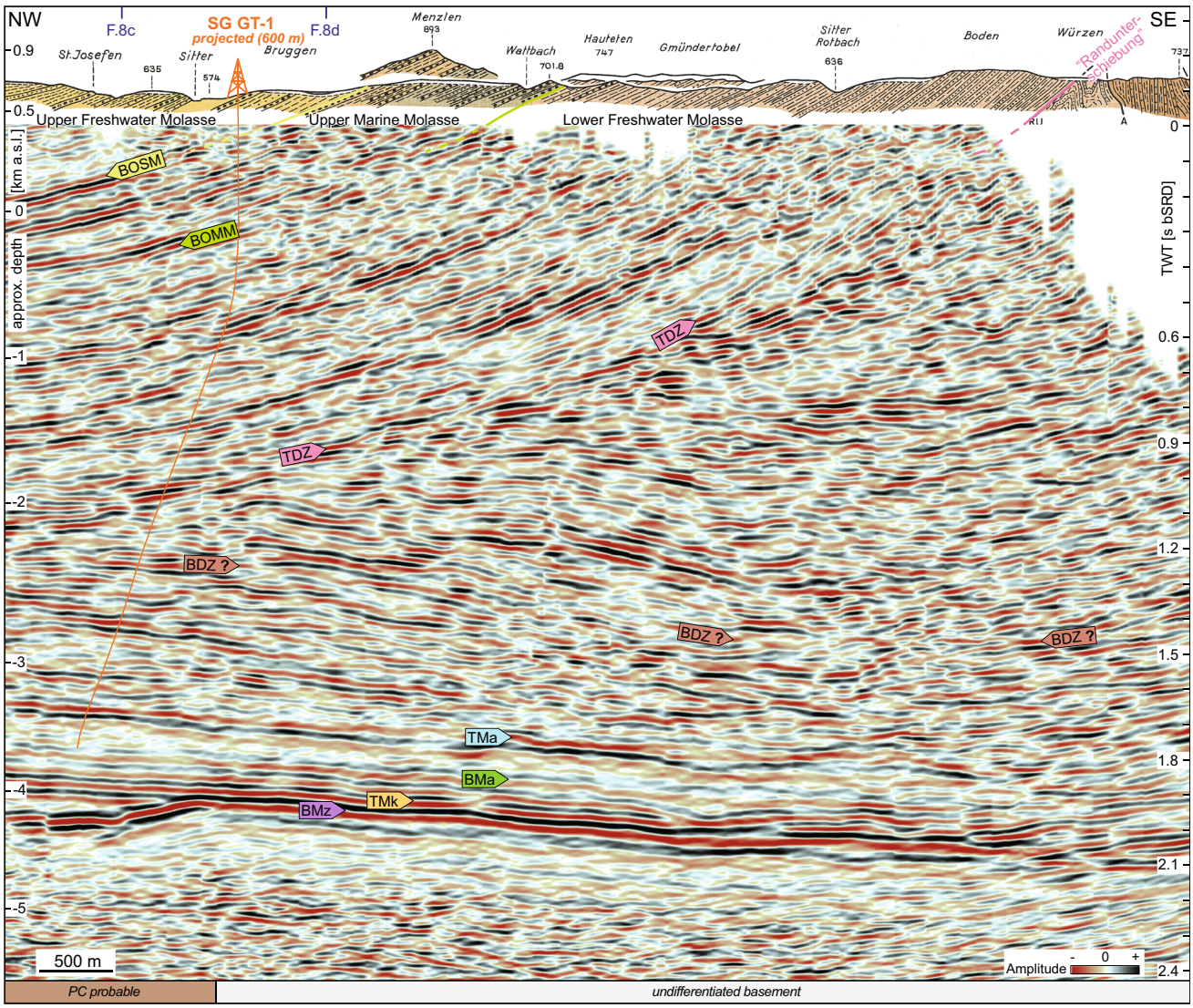


Fig. 5 3D seismic cross-section along the northern part of cross-section no. 7 published by Eugster et al. (1960) illustrating the excellent match of surface geology and 3D seismic data (see Fig. 4 for section trace). The shallow, NW dipping Molasse reflections are separated from the underlying triangle zone by the back thrust mapped as TDZ (Top Dreieckzone, i.e. "Randunterschiebung"). The borehole trajectory of SG GT-1 is projected onto the section plane over several hundreds of metres (600 m at well head, 1000 m at the bottom hole; compare with Fig. 4). The *blue tick marks* indicate the locations of the intersecting sections shown in Fig. 8c, d

rather densely populated area with pronounced topography, the quality at the level of the Cenozoic and Mesozoic reflections can generally be regarded as good to excellent. Towards the south, however, data quality decreases. This is most likely due to the increasing depth of the reflectors in the Mesozoic sequence, to imbricate thrust wedges in the triangle zone with steep reflectors distorting the seismic image, and to significantly more pronounced topography south of the city of St. Gallen (Fig. 5). Here, substantial rearrangements in the seismic excitation pattern were locally necessary and difficult acquisition conditions resulted in a shortfall of single excitation points and a loss of seismic resolution.

3.1 Interpretation of seismic horizons and faults

As no deep stratigraphic borehole data were available for seismic calibration within 25 km of the 3D seismic survey area (Fig. 1), eight seismic horizons were picked along reflections with characteristics mainly adapted from earlier 2D and 3D seismic interpretations (Roth et al. 2010; Madritsch et al. 2013) and calibrated in the deep boreholes Lindau-1, Herdern-1 and Kreuzlingen-1. The log data from borehole SG GT-1 (available only after the initial 3D seismic interpretation) reach the uppermost part of the Middle Jurassic Dogger formation and were used to compute time-linear synthetic seismograms for Ricker

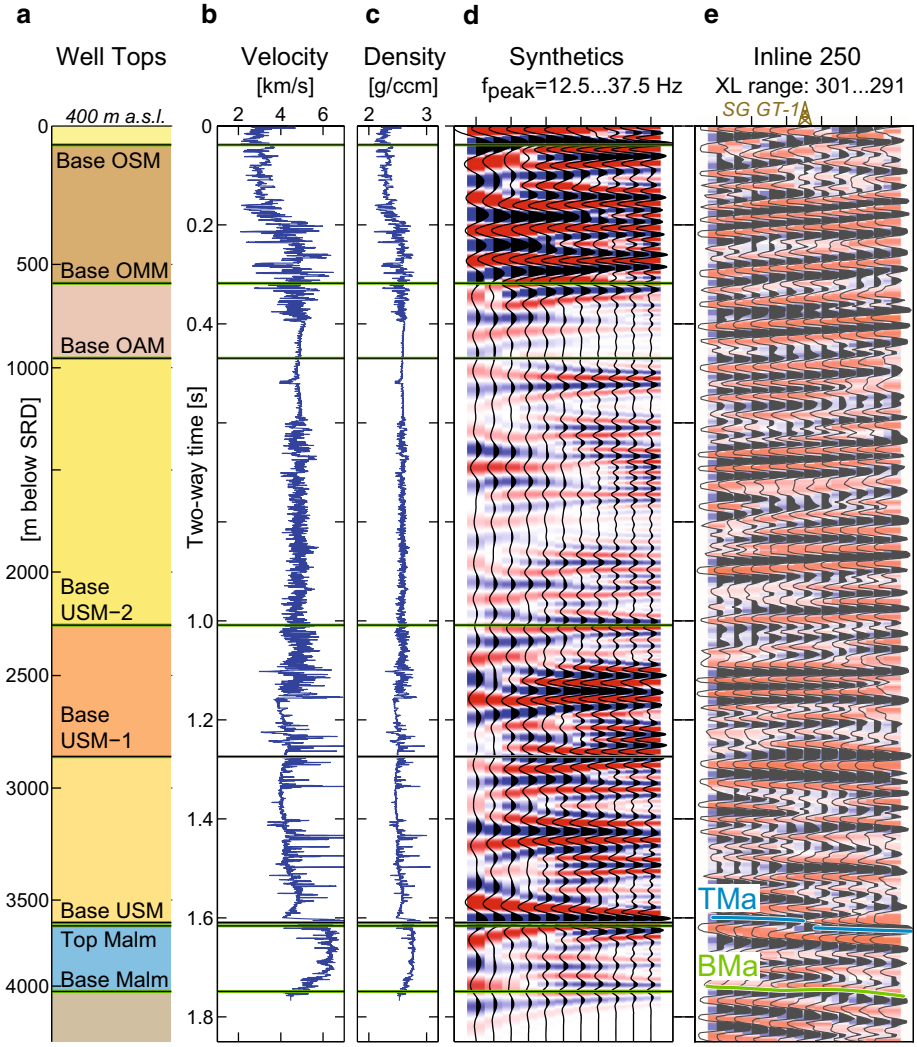


Fig. 6 **a** Non-linear depth column showing the well tops as derived from the litho-log of SG GT-1 and adjusted to the time-linear scale using the check shot corrected sonic log. Note that the seismic reference datum (SRD) is 400 m a.s.l. and that the well head (not indicated) is on 579 m a.s.l. **b** Velocity column shown as the inverse of the check-shot-corrected sonic log. The correction was only applied down to the Top Malm (TMa) horizon. **c** Density column showing densities inferred from sonic log (P-wave velocities) by the Gardner's Law (Gardner et al. 1974). Density in SG GT-1 could only be measured in the Upper Jurassic Malm section. **d** Calculated, time-linear synthetic seismograms for Ricker wavelets with different central frequencies. **e** Extract of inline (IL) 250 with crosslines (XL) ranging from 301 to 291 centred around the penetration point of SG GT-1 at Top Malm. The TMa and BMa lines correspond to the seismic horizons as interpreted in this project. Note that the polarity of the seismic section has been reversed in this figure to match the synthetic seismograms

wavelets with different central frequencies (Fig. 6). This calibration shows that at least for the Upper Jurassic Malm formation, the reflection seismic data match the borehole log data reasonably well and that the aforementioned regional seismic calibration is valid. The seismic horizons are (Figs. 3, 5): Base Upper Freshwater Molasse (BOSM), Base Upper Marine Molasse (BOMM), Top Triangle Zone (TDZ) and Base Triangle Zone (BDZ), Top Malm (TMa), Base Malm (BMa), Top Muschelkalk (TMk) and Base Mesozoic (BMz). The Cenozoic horizons were interpreted using a homogeneous grid of seed lines (SW–NE striking inlines, NW–SE striking crosslines) with a grid spacing of 500 m. TDZ and BDZ represent low-angle thrusts that were technically treated as horizons during the seismic interpretation procedure. As the focus of the seismic investigation was on the Mesozoic units and the SFZ, the interpretation there was carried out on a denser grid with 250 and 125 m spacing, respectively. In contrast to the marine Mesozoic sequence, most of the Cenozoic Molasse consists of wedge-shaped units of fluviatile continental sediments (except the comparatively thin Upper Marine Molasse) that form laterally inhomogeneous bodies and thus reveal few continuous reflections (e.g. Homewood and Allen 1981; Kempf et al. 1999). However, the two upper Molasse horizons BOSM and BOMM could be mapped with confidence and were tied (1) to their outcropping lithological contacts within the 3D seismic survey area (Eugster et al. 1960; Fig. 5), and (2) to the relevant horizons of the regional 2D seismic interpretation (Roth et al. 2010). Due to the lack of sufficiently continuous reflections, fault interpretation in the Molasse is very challenging. TDZ is an exception as it could locally be mapped by very clear discordances (Fig. 5) and is expressed in outcrops as a fault (the so-called "Randunterschiebung", Habicht 1945; Eugster et al. 1960). The essentially bedding-parallel BDZ could only be mapped tentatively. Below BOMM, no Molasse horizon was mapped.

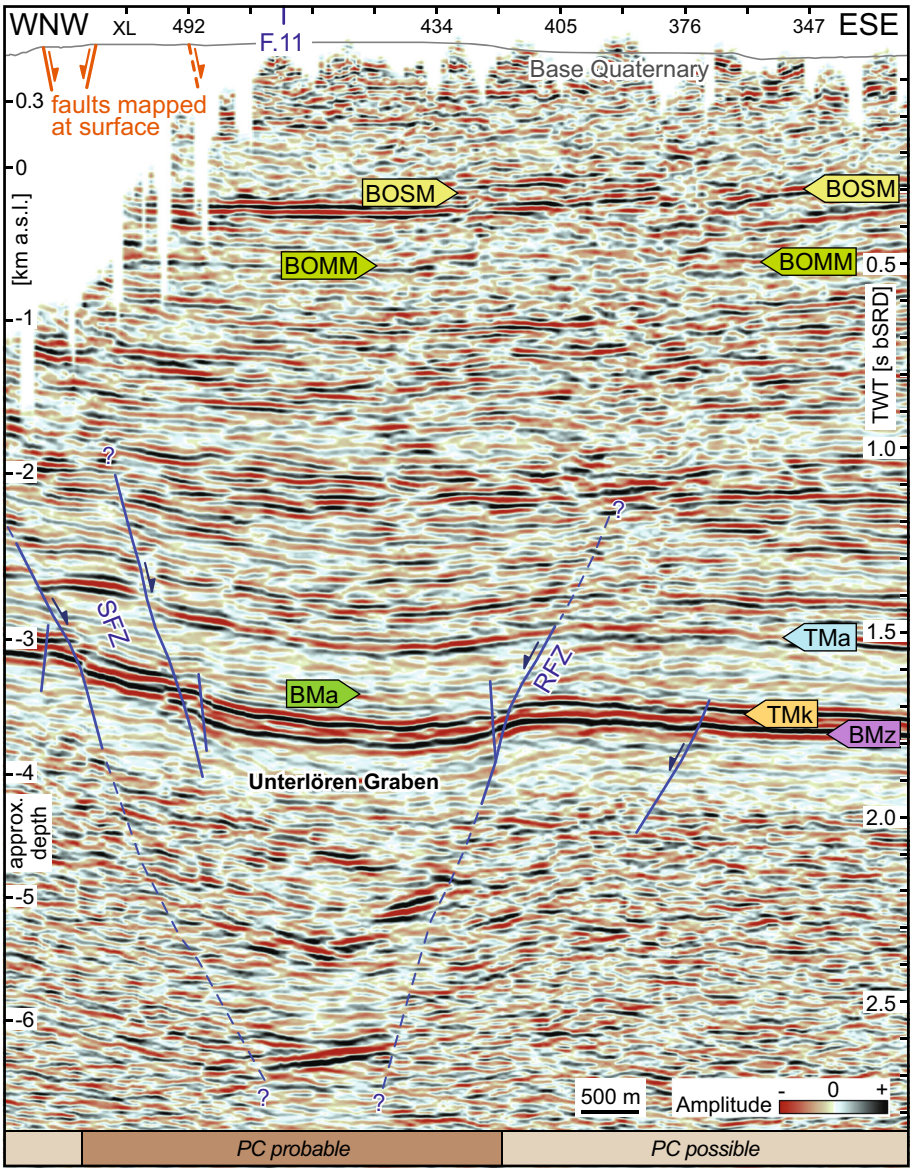


Fig. 7 Seismic cross-section across St. Gallen Fault Zone (SFZ), Unterlören Graben and Roggwil Fault Zone (RFZ) in the northern part of the area covered by 3D seismic data. See Fig. 4 for location of section trace. The Unterlören Graben is bounded by the SFZ in the WNW and the RFZ in the ESE. High-amplitude PC reflections in the basement help localising the downward continuation of the graben bounding faults. PC reflections seem to also occur up to c. 1.5 km eastward of this graben. The potential upward continuations of the SFZ and RFZ above the reflections at the level of the Mesozoic strata do not reach higher than 2.6–2.8 km below terrain (i.e. 700–800 m above TMa). No direct structural link can be made between the SFZ faults and the three faults mapped at the surface (see also map view in Fig. 4). This is either because there is no such link, or because it cannot be seen due to the laterally discontinuous nature of the Molasse deposits making fault interpretations in the Molasse units a very challenging task. In addition, this section is located at the very northern edge of the 3D seismic where seismic coverage is deficient. Further to the south, reflection offsets along the SFZ in the lowest Molasse units do not reach higher than c. 450–650 m above TMa. The *blue tick mark* indicates the location of the intersecting section shown in Fig. 11

The Mesozoic series are clearly identifiable as a prominent band of very homogeneous and continuous, yet faulted, high-amplitude reflections (Fig. 7). TMa is expressed throughout most of the survey area as a pronounced seismic reflection. We mapped the red trough (amplitude minimum) as TMa, representing the acoustic impedance increase from the soft Molasse sandstones and conglomerates to the comparatively harder Malm limestones. Locally, the TMa reflector reveals angular unconformable relationships with the overlying Molasse units (Fig. 8). The BMa horizon is not the result of a single, strong seismic reflector. The lower section of the Malm and

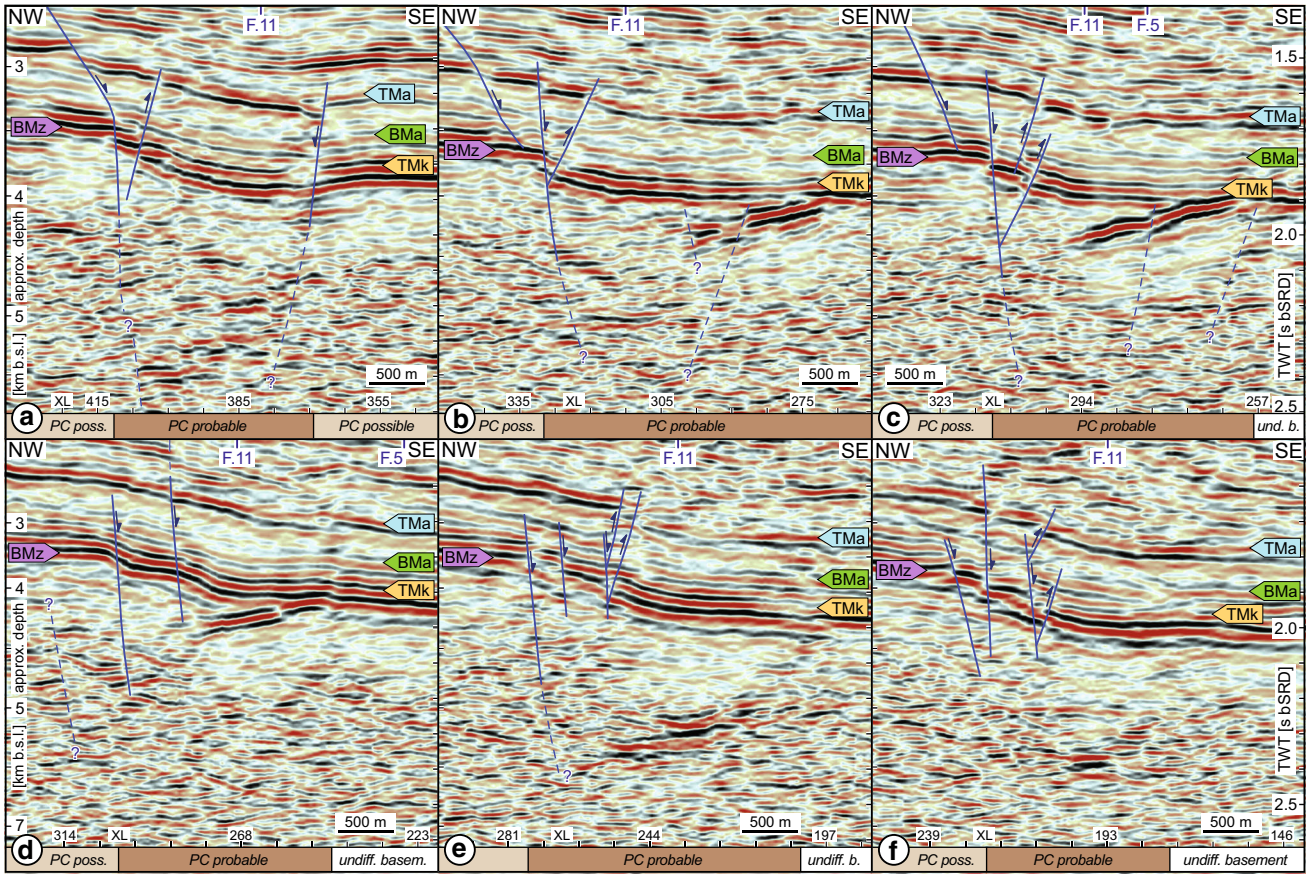


Fig. 8 Series of seismic cross-sections across the SFZ, focusing on the reflections in the Mesozoic sequence and in the pre-Mesozoic basement, arranged from north **a** to south **f**. See Fig. 4 for section traces. The *blue tick marks* indicate the locations of intersecting sections shown in Figs. 5 and 11

the uppermost section of the Dogger formations represent a rather monotonous, seismically transparent low-reflectivity zone. The BMa horizon was mapped as a zero-crossing (positive–negative). The lower Mesozoic shows large impedance contrasts and therefore reflections with higher amplitudes. The TMk horizon could be continuously mapped as a zero-crossing (positive–negative) above a strong trough. The first continuous reflection phase (a positive–negative zero-crossing) above the angular unconformities in the basement was picked as BMz. Fault interpretation at the level of the Mesozoic strata was done on the same grid of in- and crosslines as used for the horizon interpretation. This resulted in structural contour maps (Fig. 9) from which thickness maps (Fig. 10) could be calculated. For the depth conversion of the structural maps in time, a velocity model was used that is based on the processing velocities and is calibrated with the data of the check shot survey of borehole SG GT-1.

The analysis of the coherence volume enabled us to map medium-scale faults at the limit of seismic resolution (vertical displacement below c. 30 m). Location and orientation of this set of faults are consistent with most of the large-scale faults mapped by means of classical interpretation of the 3D reflection seismic data. The seismic dataset does not allow the interpretation of seismic reflections in the topmost decametres due to quaternary overburden and/or weathering of the rocks and because seismic data acquisition and processing were optimised for a deeper target (i.e. Mesozoic units).

3.2 Interpretation of pre-Mesozoic reflections

Pre-Mesozoic seismic horizons could not be mapped systematically. As observed in northern Switzerland and compared with the overlying sediments, the crystalline basement often has a seismically isotropic character (e.g. Birkhäuser et al. 2001; Madritsch et al. 2013). The primarily fluvial and lacustrine PC deposits (e.g. Matter 1987) are not laterally continuous strata and thus do not create seismic reflections traceable over long distances. However, such short seismic reflections could in some cases also arise from mylonitic shear zones in the crystalline

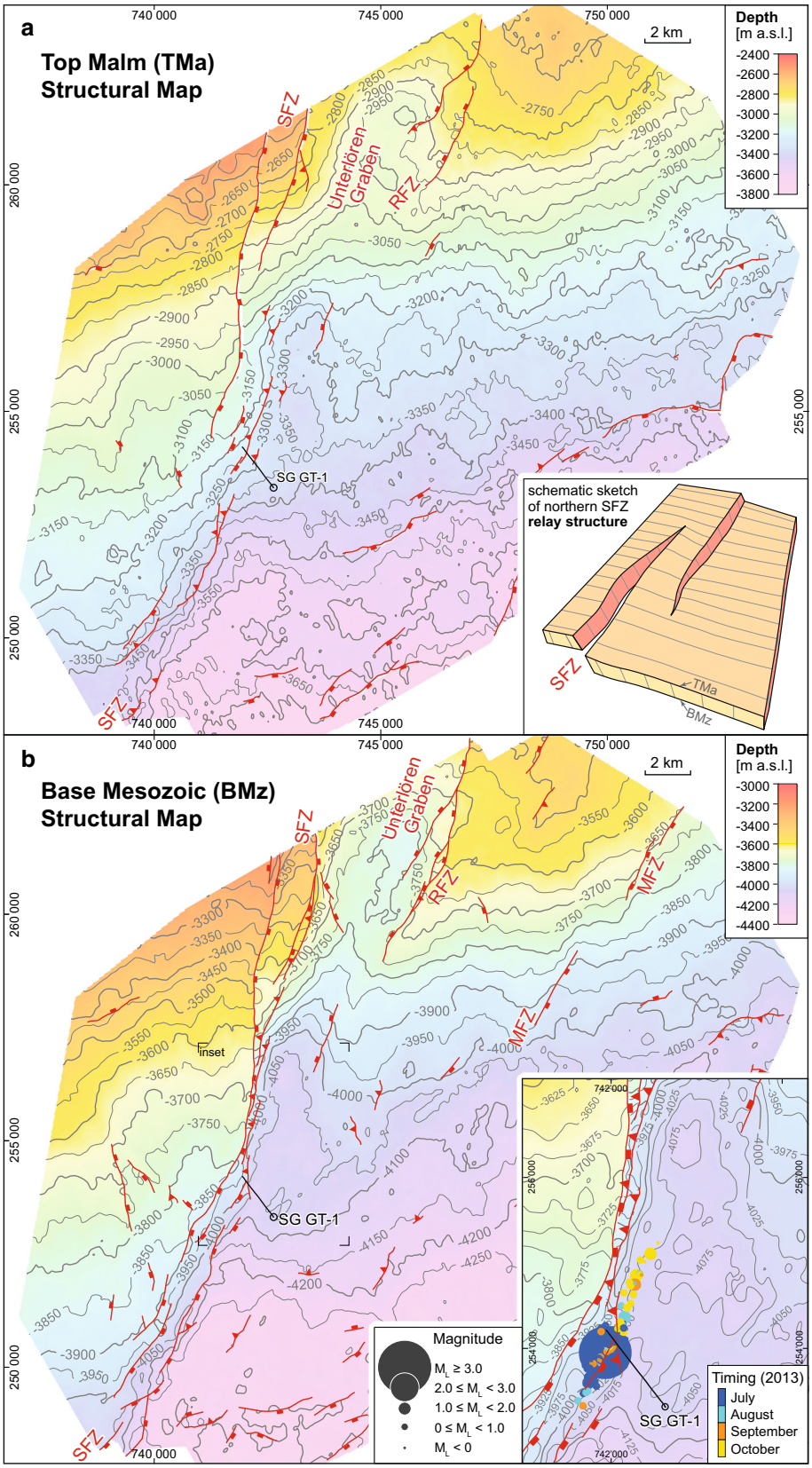


Fig. 9 Depth contour maps of TMa (**a**) and BMz (**b**). Local, narrow white stripes along the faults in the coloured depth grids represent areas over which the marker horizons are omitted by faulting. In the case of normal faults, footwall fault lines are shown, in the case of reverse faults, hanging wall fault lines are plotted. The northern part of the St. Gallen Fault Zone (SFZ) forms a relay structure (see sketch in *inset* in **a**, with a geometry modified from Rotevatn et al. 2009). The *inset* in **b** shows a zoom of the BMz map with preliminary relative relocation (Diehl et al. 2014b) of the induced seismic sequence between July and November 2013. *RFZ* Roggwil Fault Zone, *MFZ* Mörschwil Fault Zone

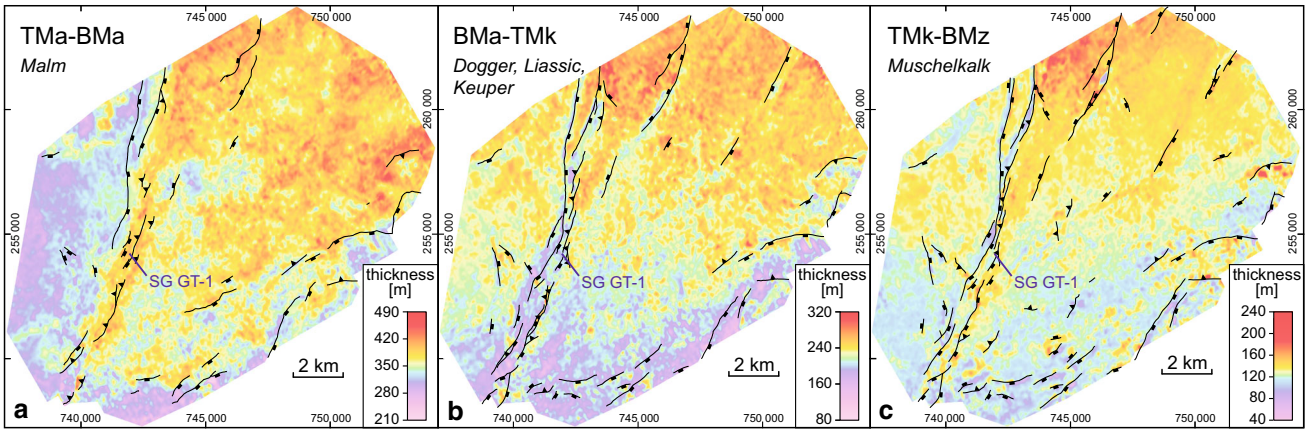


Fig. 10 Isopach maps of three Mesozoic intervals: **a** TMa-BMa (Upper Jurassic), **b** BMa-TMk (Middle and Lower Jurassic and Upper Triassic) and **c** TMk-BMz (Middle and Lower Triassic). Thickness is calculated as true vertical thickness. The faults shown are those that offset the upper horizon of each interval. All three maps reveal an abrupt increase of thickness across the SFZ, from west to east. The TMk-BMz map also shows an increased thickness within the Unterlören Graben with respect to the area east of the RFZ

basement. Both can be masked by interbed multiples (reverberations originating from the shallower levels). For basement units (crystalline and PC) in general, seismic imaging is also poorer because of the great depths (i.e. long ray paths) that lead to attenuation of the higher frequency components. Finally, the amplitude gain control (AGC) operators selected by the processing company were optimised to highlight the very high reflectivity of the Mesozoic sediments (the main target of the geothermal exploration study) with the disadvantage of creating a shadow zone underneath.

The seismic data set available is not the result of a true-amplitude processing. Several processing steps (like migration, filtering or AGC) do alter the integrity of absolute amplitude values. Yet, using specific reflection characteristics, a tentative mapping of PC deposits was performed (for more details on possible criteria see e.g. Marchant et al. 2005; Naef and Madritsch 2014). Local packages of high-amplitude reflections as well as reflections that are discordant to the BMz could be identified (Figs. 5, 8, 11). Similar high-amplitude reflection packages are documented in 2D seismic sections in central northern Switzerland (Sprecher and Müller 1986; Nagra 2008; Naef and Madritsch 2014) where they are proven to represent the seismic expression of Carboniferous (Stephanian) coal units as evidenced in the borehole Weiach-1 (Matter 1987; Nagra 1989).

To support the classical interpretation along seismic vertical sections or time slices, we calculated root mean square (RMS) attributes (e.g. Chopra and Marfurt 2007) and displayed them in map view (Fig. 12). By highlighting areas with anomalously high or low amplitudes, these maps allowed us to further narrow down possible PC occurrences. For these attribute maps, a time interval relative to a mapped horizon has to be specified, within which amplitude information is extracted (Fig. 12).

4 Structural interpretation

4.1 The SFZ geometry at the level of the Mesozoic strata

The 3D seismic interpretation clearly revealed that the SFZ forms a prominent NNE–SSW striking fault zone composed of steeply ESE dipping normal faults with subsidiary, subparallel apparent reverse faults in the hanging wall (Figs. 8, 9). The fault zone can be divided into a northern, c. N10-20°E striking and a southern, c. N30°E striking part, the transition between the two being located about 2 km northwest of the SG GT-1 borehole surface location (Fig. 9). The northern part is dominated by two continuous normal faults forming a relay structure (e.g. Walsh et al. 1999; Conneally et al. 2014; Fig. 9a inset) that likely extends outside of the investigated area further to the north. The offset of the BMz horizon along the eastern normal fault continuously increases from the fault tip towards the NNE reaching c. 290 m (180 m at TMa) in the very north of the survey area. At the western normal fault, the BMz offset amounts to 80 m in the very north (70 m at TMa) and increases towards the SSW to reach 180 m (100 m at TMa) in the area of the termination of the eastern normal fault. These two normal faults represent the western bounding faults of a NNE–SSW striking graben (termed here the Unterlören Graben) that widens towards the NNE (Fig. 9). It is bounded to the east by a zone of NW dipping normal faults termed here the Roggwil Fault Zone (RFZ).

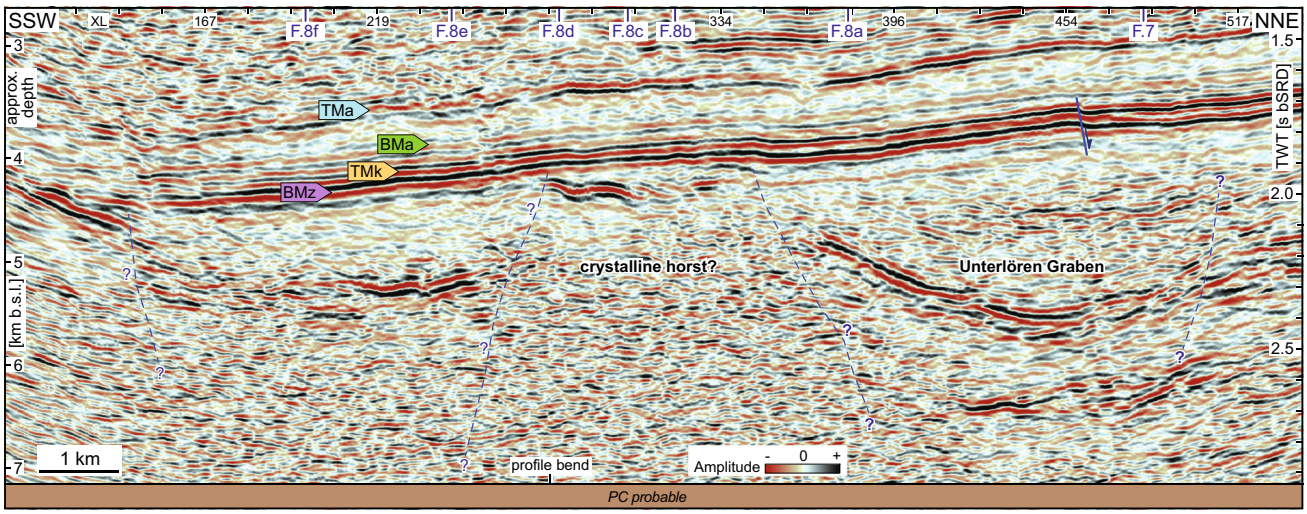


Fig. 11 Seismic cross-section oriented along strike and located in the hanging wall of the SFZ (see Fig. 4 for section trace). The PC reflections display two areas of rather continuous, synformal reflection bands in the pre-Mesozoic basement, interpreted as PC graben elements, separated by a (seismically more transparent) crystalline horst topped by a very thin band of reflections interpreted as PC sediments (compare with Fig. 12b, d). The pre-Mesozoic fault segments could only be tentatively mapped. The discontinuous seismic reflections in the lower Mesozoic at approximately XL 150 are regarded as the result of poorer seismic imaging and not as indicating the presence of a fault. The *blue tick marks* indicate the locations of the intersecting sections shown in Figs. 7 and 8a–f

In the southern part of the SFZ, offsets across individual faults are less pronounced. Laterally continuous normal faults are less numerous, comparatively shorter and offset the Mesozoic seismic horizons less than 130 m. However, flexures (e.g. Withjack et al. 1990) in the Mesozoic strata point to underlying normal faults within the basement that still may have substantial offsets (Fig. 8d–f). The subsidiary subvertical apparent reverse faults in the hanging wall of the SFZ are interpreted as typical hanging wall features of a convex-upward normal fault (e.g. Mandl 2000). They are thus not regarded as the result of a regional compression but rather relate to the extension that produced the SFZ major normal faults.

Further east, there is a c. 15 km long zone of subvertical, SW–NE striking normal faults termed here Mörschwil Fault Zone (MFZ). The fault segments, expressed only in the lower half of the Mesozoic sequence, form a left-stepping en échelon array from NE to SW. (Fig. 9b). The MFZ is also visible in the RMS amplitude map covering the lower half of the Muschelkalk formation (Fig. 12a). This could be the expression of different seismic responses from the lower halves of the Muschelkalk subunits on both sides of the MFZ due to subtle differences in thickness across the fault zone (Fig. 10c).

4.2 The SFZ at the level of the Cenozoic deposits

The SFZ and RFZ can be vertically traced only up to c. 1.1–1.2 s TWT below SRD (corresponding to c. 2.6–2.8 km below terrain) across the overlying Molasse units in the very north of the 3D seismic survey area (Fig. 7). There, published geological maps (Hofmann 1951; Saxer 1964; Hofmann 1973) reveal clear offsets of conglomeratic key horizons in the Sitter Valley c. 4 km northeast of Waldkirch (see "surface geology" faults in Fig. 4 and "faults mapped at surface" in Fig. 7). These normal faults, confirmed by our own field observations, strike parallel to the SFZ. Due to poor outcrop conditions, their mappable extension amounts to a few hundred metres only. In the seismic data, the lack of shallow coverage in this border area of the 3D survey (Fig. 7) precludes their identification. At greater depth, the SFZ offsets Molasse reflections in the lowermost 700–800 m. No direct structural link can thus be made between those offsets at depth and the three faults mapped at the surface. This is either because there is no such link, or because it cannot be seen due to the laterally discontinuous nature of the Molasse deposits making fault interpretations in the Molasse units a very challenging task, in particular when seismic coverage is limited. Further to the south, reflection offsets along the SFZ in the lowest Molasse units do not reach higher than c. 450–650 m above TMa.

4.3 The SFZ to the north of the 3D seismic survey

Available 2D seismic lines located north of the St. Gallen 3D seismic survey also display E dipping normal faults at the level of the Mesozoic strata (Roth et al. 2010; Sommaruga et al. 2012). They represent the northern extension

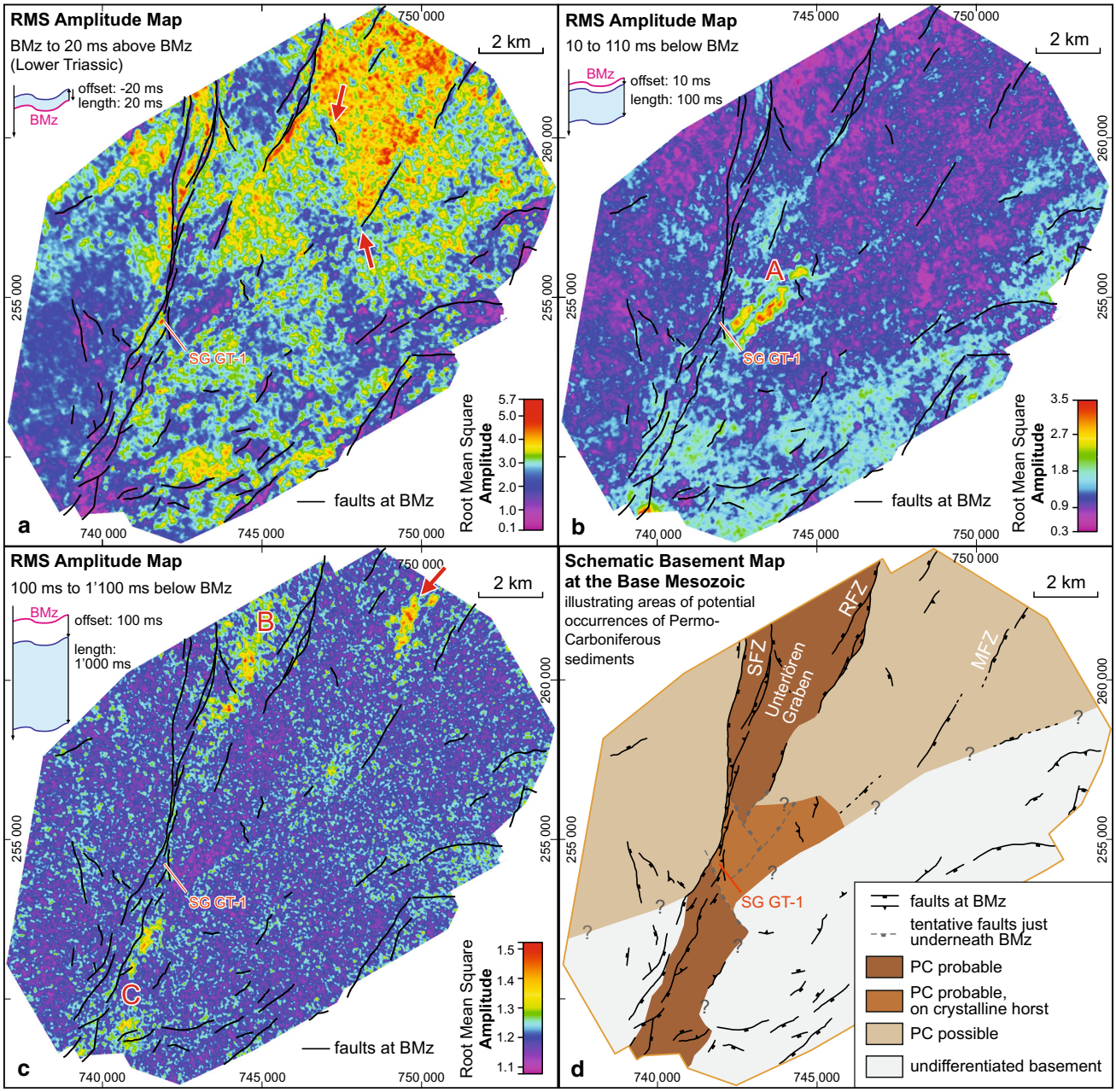


Fig. 12 **a**–**c** Attribute maps of root mean square amplitudes above and below BMz. The maps show the results of amplitude extractions within certain observation windows with high amplitudes in *red* and *yellow* and low amplitudes in *dark blue* and *purple*. The relevant amplitude extraction window is characterised by its "offset" from BMz (positive in downward direction) and its "length" (vertical extent), both specified in two-way travel time. Note that the schematic sketches of the observation window dimensions at the top left of the figures are not to scale. **a** 20 ms thick window directly above BMz. The main structural features (SFZ, RFZ, Unterlören Graben, MFZ) are clearly highlighted by significant contrasts in amplitude. Note the NNW–SSE striking change of amplitudes east of the Unterlören Graben between the northern termination of the RFZ and the MFZ (marked by two *red arrows*). **b** 100 ms thick window at 10 ms underneath BMz. Note the SW–NE striking, high-amplitude anomaly (A) directly northeast of SG GT-1. This anomaly marks the PC reflections on the assumed crystalline horst discordantly underlying BMz (see also Figs. 8b–d and 11). **c** 1000 ms thick window at 100 ms underneath BMz encompassing three areas with probable PC reflections (*B*, *C* and a fourth one marked by the *red arrow*). **d** Interpretative structural map of the basement at the level of BMz (i.e. top basement) highlighting the areas of probable and possible PC occurrences. These areas are compiled from **b**, **c** and the interpretation of vertical reflection seismic sections. Note that the distinction between the areas designated as "PC possible" and "undifferentiated basement" is rather speculative

of the SFZ (Figs. 1, 4). At the level of the Cenozoic deposits, however, the situation is less clear. The at least 1 km long and NNW–SSE to NW–SE striking, NE dipping normal faults southeast of Amriswil (Fig. 4), mapped at the upper Cenozoic horizons BOSM and BOMM (>1800 m above TMa), do not represent compelling evidence for the upward continuation of the SFZ (mapped at the level of the Mesozoic strata). A more detailed consideration of the lower part of the Cenozoic sequence is not possible as there are no other seismic horizons available between BOMM and TMa (Roth et al. 2010).

Still further to the NNW, c. 5 km west of Romanshorn (Fig. 1), a major NE dipping normal fault (termed here Dozwil Fault, Fig. 4) offsets the entire Mesozoic section by up to c. 270 m and extends upwards to the uppermost Upper Freshwater Molasse (Roth et al. 2010; Sommaruga et al. 2012). In contrast to the SFZ, the Dozwil Fault also offsets almost the entire Cenozoic sequence. It strikes NW–SE and is interpreted on the basis of two 2D seismic lines only. Note that the SFZ (at the level of the Mesozoic strata) was regarded as being linked to the Dozwil Fault in earlier interpretations (Roth et al. 2010). However, geomechanically such an anticlockwise bend of the faults' strike does not make sense. We interpret the Dozwil Fault as not being linked to the SFZ because of the different strike of the two faults and because of the very different extents and geometries at the level of the Cenozoic units although offsets at the level of the Mesozoic units are very similar.

4.4 Synsedimentary faulting along the SFZ

Isopach maps of three Mesozoic intervals, namely Upper Jurassic (TMa-BMa, Malm), Middle-Lower Jurassic and Upper Triassic (BMa-TMk, Keuper–Liassic–Dogger) as well as Middle-Lower Triassic (TMk-BMz, Muschelkalk), show that the (vertical) thicknesses of these three intervals steadily decrease towards the SSE (Fig. 10). A significant thickness increase exists across the northern part of the SFZ, from WNW towards ESE. There, the Malm formation interval is c. 330 m thick in the footwall and c. 340–420 m in the hanging wall, i.e. the Unterlören Graben. In the borehole SG GT-1 (located south of the Unterlören Graben), the drilled Malm section is 398 m thick (true vertical depth thickness). The thickness of the Keuper–Liassic–Dogger sequence increases from c. 230 m in the footwall of the SFZ to c. 280–310 m in the Unterlören Graben. The thickness increases in these two intervals correlate with a clear change of seismic facies across the SFZ, from continuous reflections in the footwall to significantly less continuous reflections in the hanging wall. The Muschelkalk interval reveals a less pronounced thickness anomaly in the Unterlören Graben. The thickness increases from c. 130 m in the footwall of the SFZ to 140–190 m in the hanging wall. East of the RFZ it reaches c. 130–160 m. As compared to the aforementioned intervals, the Muschelkalk interval shows only gentle seismic facies changes. The distinct amplitude change in the lower half of the Muschelkalk formation along a NNW–SSE striking zone between the northern termination of the RFZ and the MFZ (Fig. 12a) might point to another change in seismic facies.

The observed thickness changes demonstrate that the SFZ and the RFZ must have been active throughout the Mesozoic. Subsidence in the Unterlören Graben was most pronounced during Early-Middle Triassic times pointing to synsedimentary activity particularly along the northern part of the SFZ and the RFZ. This early synsedimentary activity clearly points to the existence of basement-rooted faults that probably reactivated older faults related to the formation of the Permo-Carboniferous grabens. The cross-section across the Unterlören Graben (Fig. 7) illustrates how the SFZ and RFZ can be tentatively mapped in the basement. During Late Triassic and Jurassic times, normal faulting was restricted to the SFZ.

4.5 Attribute maps as possible indicators of Permo-Carboniferous sediments

Attribute analyses and local seismic interpretation show that high-amplitude reflections with significant (>1 km) lateral continuity exist in the pre-Mesozoic basement. These reflections primarily occur in areas located in the hanging wall of the SFZ, e.g. in the Unterlören Graben. They are interpreted as pointing to the presence of PC sediments. Attribute maps of the basement reveal three areas adjacent to the SFZ with amplitude anomalies at various depths: (a) a SW–NE striking area directly northeast of SG GT-1 (Fig. 12b), (b) an SFZ-parallel, elongated area within the Unterlören Graben (Fig. 12c), and (c) an SFZ-parallel area to the south of SG GT-1 (Fig. 12c). Anomaly A is the most pronounced anomaly and strikes obliquely to the SFZ. In Figs. 8b–d and 11 it appears as an inclined high-amplitude reflection band just underneath the BMz reflections. These reflections are interpreted to be located on top of a crystalline horst structure (Fig. 11) and might be indicative for a hydrocarbon-bearing sedimentary unit discordantly underlying the Mesozoic sequence. Anomaly B encompasses two high-amplitude reflection bands at different levels (Fig. 11): at c. 2100–2450 ms and at c. 2700 ms below SRD (c. 4650–5700 m and c. 6450 m b.s.l.); the shallower one displays a synformal structure. In the section in Fig. 7, perpendicular to the section in Fig. 11, this upper high-amplitude reflection band also shows a synformal geometry. Anomaly C points to a similar synformal high-amplitude reflection band with the same orientation as the shallower one in Anomaly B. A fourth amplitude anomaly area is located east of the

Unterlören Graben and is best illustrated in the sampling window at 100–1100 ms below BMz (Fig. 12c). This anomaly trends NNE–SSW and strikes subparallel to the neighbouring RFZ and MFZ. In contrast to the other three anomalies, the high-amplitude reflections of this fourth one cannot be related to major faults that would represent graben bounding structures.

Mapping the discrete patches of high-amplitude reflections bands at different levels below the BMz enabled us to identify local areas of "probable" and areas of "possible" PC sediment occurrences (Fig. 12d). The results show that PC sediments are very likely present in the Unterlören Graben and also in the hanging wall of the southern part of the SFZ. This coincides with the areas for which a graben structure can be inferred by the seismic data at the level of the Mesozoic strata. We can thus conclude that the SFZ and the RFZ represent faults that root in the basement.

5 Neotectonic activity

The seismic activity in the area is reported to be low and diffuse (Wiemer et al. 2009; Diehl et al. 2014a; Fig. 13). Fault plane solutions show that the stress field in northeastern Switzerland is characterised by strike-slip to normal faulting (Kastrup et al. 2004). The principal axis of horizontal compression, S_{Hmax}, is oriented NNW–SSE (c. N10°W, Reinecker et al. 2010; Heidbach and Reinecker 2013), with $S_{Hmax} > S_V > S_{hmin}$. Because the individual fault segments of the SFZ and RFZ strike at angles of between 15° and 50° to the present S_{Hmax}, many are oriented favourably for reactivation in sinistral strike-slip mode.

The installation of a dense seismic monitoring network in the framework of the St. Gallen Geothermal Power Plant Project made it possible to record seismic events down to magnitude M_L −1.0 in the vicinity of the borehole SG GT-1 (Edwards et al. 2015). On 28th June 2012, more than 1 year before the start of the drilling operations, a natural seismic event with M_L 2.1 was recorded very close to the RFZ at an approximate depth of 5.8 km. The derived fault plane solution (Diehl et al. 2014b) shows NE–SW and NW–SE striking, subvertical nodal planes, one of them striking parallel to the RFZ (Fig. 13b). On 20th July 2013, a M_L 3.5 earthquake (i.e. the main shock) and a M_L 2.1 event occurred in the vicinity of the borehole (Diehl et al. 2014a; Edwards et al. 2015). After injection tests and acid stimulation carried

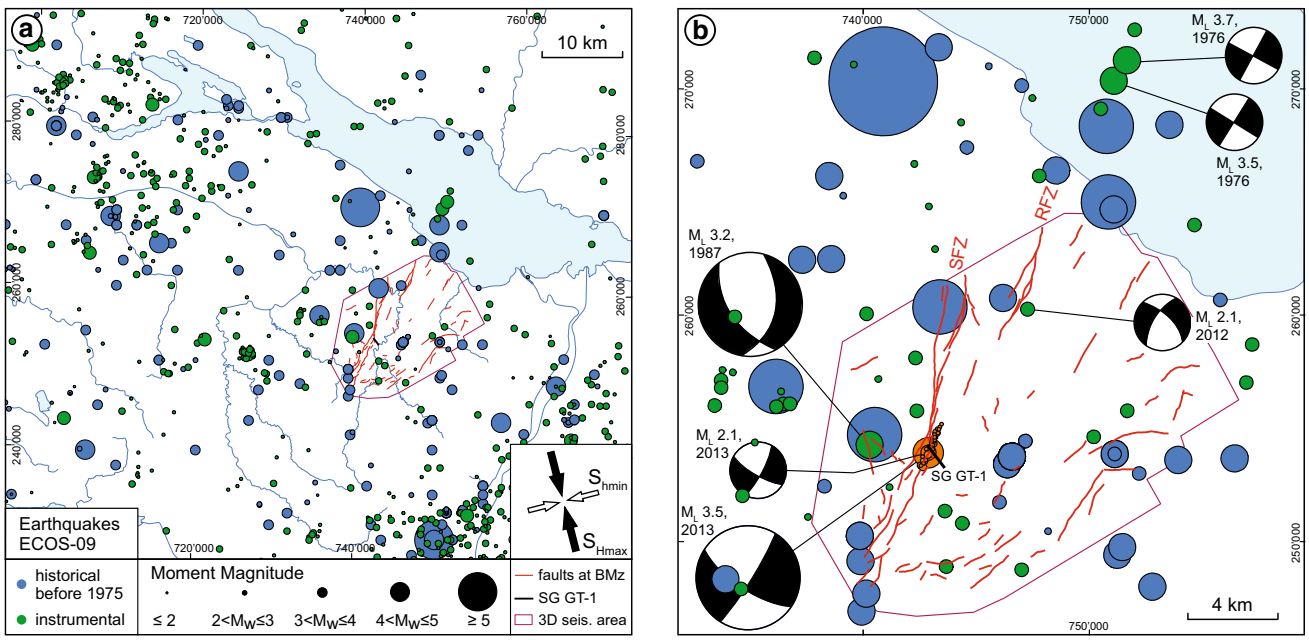


Fig. 13 **a** Distribution and magnitudes of earthquakes recorded in northeastern Switzerland according to ECOS-09 (Fäh et al. 2011). This catalogue comprises seismic events between the year 1065 and June 2009. S_{Hmax} and S_{hmin} orientations are after Heidbach and Reinecker (2013). **b** Zoom of the same dataset as in **a**, but with the induced 2013 sequence in orange and all available fault plane solutions of the area. Note the natural M_L 2.1 event of 2012 close to the RFZ. The (superposed) *orange circles* represent preliminary relative relocations of the sequence induced at borehole SG GT-1 in 2013 according to Diehl et al. (2014b). The fault plane solution of the M_L 3.5 event is according to Diehl et al. (2014a), the two M_L 2.1 events are according to Diehl et al. (2014b), the M_L 3.2 event is according to Deichmann (1990) and the ones in Lake Constance are according to Pavoni (1980)

out in the well between 14th and 17th July, gas, primarily methane most likely from a Mesozoic or sub-Mesozoic fracture reservoir along the SFZ, suddenly entered the borehole. To fight this gas kick, heavy drilling fluid was pumped into the borehole that must have increased pore fluid pressure to a level sufficient to critically reduce the shear strength of a fault and trigger the main shock and indirectly the sequence of aftershocks. The two main earthquakes occurred on subvertical fault planes (Diehl et al. 2014a; Edwards et al. 2015). The moment tensor solutions, together with the distribution of the aftershock sequence, show almost pure sinistral strike-slip motion on NNE–SSW striking nodal planes (Diehl et al. 2014b; Fig. 13b). Preliminary relative relocations by Diehl et al. (2014b) indicate that the aftershock seismicity, consisting of more than 850 events with local magnitudes between −1.7 and 2.1, was constrained to a c. 800 m long and c. 500 m thick zone at the transition of the northern (NNE–SSW striking) to the southern (NE–SW striking) section of the SFZ. According to the fault interpretation of the 3D seismic data and to the location of Diehl et al. (2014a, b), the main shock occurred at the intersection of a N–S striking reverse fault with a NNE–SSW striking normal fault (Figs. 9b inset, 13b). Local stresses were possibly highest at this fault intersection. By using a velocity model entirely derived from arrival times of a subset of the induced earthquakes, Diehl et al. (2014b) found the focal depths to be between 3.6 and 4.0 km (b.s.l.), thus in the lower part of the Mesozoic sediments. However, the differences between this velocity model on the one hand and the directly measured check shot data of borehole SG GT-1 on the other hand are significant. Therefore, hypocentre depth uncertainty remains important and a location of the induced earthquake swarm in the basement can certainly not be ruled out.

The aftershock sequence located NNE of the main shock, trending NNE–SSW, is aligned parallel to the faults at the level of the lower Mesozoic strata. However, the hypocentres do not plot directly on the mapped faults delineated in the reflection seismic data (see also Diehl et al. 2014b). But they are aligned along a NNE–SSW trending narrow zone that seems to represent a supposedly northeastern extension of the southern SFZ, connecting further northeast with the RFZ (Fig. 9b). A detailed re-evaluation of the seismic interpretation, performed after the induced earthquake series, did not reveal any BMz offset in that area. This is possibly due to faults not traceable in reflection seismic data, because of too small vertical offsets (<30 m), or because they may simply be of pure strike-slip character (and hence cannot be resolved by the seismic data in the case of subhorizontal reflections).

6 Discussion

6.1 Northern termination and Late Cenozoic to recent activity of the SFZ

Combining the fault interpretation of this study with existing 2D seismic fault interpretations (Roth et al. 2010; Sommaruga et al. 2012), the SFZ can be extrapolated towards Lake Constance at the level of the Mesozoic strata. In the area near Romanshorn, it is unclear whether the SFZ and RFZ terminate or whether they continue further northward across Lake Constance into the area near Tettnang (Fig. 1). There are no offsets in the Middle to Upper Cenozoic sequence that could be related to the SFZ, which itself is mapped at the level of the Mesozoic and lowermost Cenozoic strata (i.e. lower Oligocene, Figs. 4, 7). The two NNW–SSE to NW–SE striking faults mapped in the upper Molasse (BOSM and BOMM) north of the 3D seismic survey (Roth et al. 2010; Fig. 4) cannot be directly linked with the SFZ due to their geometry (i.e. comparatively short fault segments and different strike). However, they could be part of the Hegau-Lake Constance Graben system.

The NW–SE striking Dozwil Fault located further northwest, offsetting the entire Mesozoic and almost the entire Cenozoic sequence, possibly represents the southeasternmost segment of the Hegau-Lake Constance Graben system (Fig. 1). It remains unclear how the northern tip of the SFZ (east of Amriswil, at the level of the Mesozoic strata, Fig. 4) and the Dozwil Fault interact geometrically and kinematically. However, since the Dozwil Fault strikes parallel to the Hegau-Lake Constance Graben faults, it possibly provided a kinematic link between the Unterlören Graben and the Hegau-Lake Constance Graben during Miocene extension (Ziegler and Dèzes 2007). Madritsch (2015) infers both NE–SW and NW–SE oriented extension from paleostress data at the border of the Hegau-Lake Constance Graben. According to his interpretation, tectonic activity of the Hegau-Lake Constance Graben started after the Early Miocene and lasted until at least Late Miocene times. In this regard, the two NNW–SSE to NW–SE striking normal faults in the upper Molasse sequence (southeast of Amriswil, Fig. 4) could also be a result of this NE–SW Miocene extension rather than be a part of the SFZ.

The distribution of earthquakes in the Lake Constance area to the NNE of the St. Gallen 3D seismic survey (Fig. 13) does not allow for an allocation of these events to one of the two discussed fault systems. The localisation of the two 1976 events underneath the lake must be regarded as less precise than the localisations of other, more recent earthquakes, both laterally and vertically. Nevertheless, the pure strike-slip faulting regime would fit both to a sinistral SFZ or to a dextral Hegau-Lake Constance Graben fault

(e.g. compare with the Singen earthquake series 1995–1996 with magnitudes up to 3.3 at c. 8–9 km depth revealing a dextral strike-slip faulting regime, Deichmann et al. 2000).

Interestingly, NNE–SSW striking faults parallel to the SFZ are not observed in the northeastern NAFB west of Lake Constance (e.g. Nagra 2008; Naef and Madritsch 2014). However, further southeast, the Sax-Schwende and the supposed Rhine Valley Faults (Pfiffner et al. 2010) are major faults in the Mesozoic cover with an orientation similar to that of the SFZ (Fig. 1); but it is regarded as unlikely that these faults also root in the basement. Across Lake Constance, in the Ravensburg–Tettnang area, seismically mapped faults at the level of the Upper Jurassic units (e.g. Volz 1957; Bachmann et al. 1982) have orientations similar to that of the SFZ and RFZ (Fig. 1). Further to the northwest, the Albstadt Shear Zone represents another example of a seismogenic, NNE–SSW striking, sinistral strike-slip fault zone (Reinecker and Schneider 2002; Reicherter et al. 2008). Although recent seismicity is only recorded in the area of Albstadt (65 km NNE of Schaffhausen), Reicherter et al. (2008) speculate that the Albstadt Shear Zone might extend from Stuttgart in the north to the Hegau-Lake Constance area in the south.

6.2 Late Paleozoic to Mesozoic activity of the SFZ

The identified PC reflections along the SFZ indicate a pre-Mesozoic stage of extension across the SFZ that produced synsedimentary grabens of Late Paleozoic age. The Unterlören Graben with its bounding faults, SFZ and RFZ, strikes NNE–SSW. However, as shown by the section parallel to the SFZ (Fig. 11), a graben bounding fault probably also exists in the SSW, at the border with the assumed crystalline horst (Fig. 12d). This fault, which has no expression at the level of the Mesozoic strata, strikes obliquely (or perpendicular) to the SFZ. This southern graben border is also indicated by the shallower high-amplitude reflection band that shows a synformal geometry in NNE–SSW direction (Fig. 11). The delineation of the probable PC occurrences further to the south, south of the assumed crystalline horst, is significantly less constrained by well expressed graben bounding faults. While the high-amplitude reflections are most prominent in a 2–3 km wide zone in the hanging wall of the SFZ, PC occurrences (especially at shallower levels than in the Unterlören Graben) outside this area cannot be excluded. The southern, NE–SW striking border of the area covering these "possible" PC occurrences (Fig. 12d) has to be regarded as highly uncertain.

This study shows that short segments of PC grabens along and near the SFZ strike NNE–SSW and thus obliquely to the general PC grabens trend in northeastern Switzerland (Diebold et al. 1991; Marchant et al. 2005; Naef and Madritsch 2014). On the other hand, NNE–SSW striking PC graben structures are common in the Helvetic Alps and cover a large area within Central Europe (e.g. Ziegler and Dèzes 2006). Ziegler (1990) postulated major, pre-Permian faults in the basement of Central Europe that strike WSW–ENE, WNW–ESE and NNE–SSW.

Thickness differences across the Unterlören Graben in the Lower and Middle Triassic units imply normal faulting activity along the SFZ and the RFZ. We found no seismic indications for a Late Triassic inversion phase as suggested by Marchant et al. (2005) for the Benken 3D seismic survey area and areas further WNW. In the two upper Mesozoic intervals, an increase in thickness can be documented only across the SFZ, implying continued or repeated extension during Late Triassic to Late Jurassic times. As only four Mesozoic horizons have been mapped, a more precise temporal resolution of synsedimentary activity could not be achieved. Marchant et al. (2005) postulated a "sharp subsidence event" for this period, which they compiled from subsidence curves from several boreholes in northern Switzerland. The observed changes in seismic facies of the Late Triassic to Late Jurassic strata above the PC Unterlören Graben likely represent lithofacies variations. The variations in thickness of the Upper Jurassic deposits across the SFZ can be explained in two ways. Either this change is due to synsedimentary subsidence east of the SFZ, or alternatively, the area west of the SFZ was uplifted and eroded during the Cenozoic. The latter would be related to the developing forebulge in the Molasse basin during Alpine convergence (Crampton and Allen 1995; Schlunegger et al. 1997). However, the combination of both a change in thickness and a change in seismic facies points to the first scenario. Both phenomena are reported also from northwestern Switzerland: major Mesozoic synsedimentary faulting is postulated to have occurred during Middle Jurassic times (e.g. Burkhalter 1996), as are facies and thickness changes during Late Jurassic times (Allenbach and Wetzel 2006; Meier and Deplazes 2014). The thickness increases of the Lower and Middle Triassic units above the Unterlören Graben and the significant thickness increase of the Upper Triassic to Upper Jurassic units across the SFZ from west to east are thus interpreted as indicators for continuous or repeated phases of extension and related subsidence during the Mesozoic. This extension reactivated former basement-rooted faults that were already active in Late Paleozoic times.

7 Conclusions

The detailed interpretation of the St. Gallen 3D seismic dataset revealed a prominent NNE–SSW striking structure, the St. Gallen Fault Zone. The fault zone comprises ESE dipping normal faults with subsidiary, subparallel apparent

reverse faults in the hanging wall. It offsets the entire Mesozoic sequence by up to 300 m. The offsets in the overlying Cenozoic deposits are not reliably resolvable within the 3D seismic area, but, if present, they are very likely significantly smaller. Further to the north, faults are documented that do indeed offset the upper Cenozoic units. However, their geometry implies that they are decoupled from the St. Gallen Fault Zone elements at the level of the Mesozoic strata. Moreover, those faults, together with the NW–SE striking Dozwil Fault further to the north, more probably are part of the Hegau-Lake Constance Graben active during Miocene extension.

Significant thickness changes across the St. Gallen Fault Zone illustrate repeated synsedimentary activity of the fault zone during the Mesozoic. The St. Gallen and the Roggwil Fault Zones delimit a NNE–SSW trending Mesozoic and Permo-Carboniferous graben system in the hanging wall. These faults belong to a set of central European basement faults that likely formed during a post-Variscan, Late Paleozoic phase of dextral transtension. During the Mesozoic and the early Oligocene, the St. Gallen Fault Zone was repeatedly reactivated in normal faulting mode. Recent natural and induced earthquakes show that the St. Gallen Fault Zone is presently active in sinistral strike-slip mode, favoured by its almost ideal fault orientation within the present-day stress field.

Acknowledgments The authors thank the Sankt Galler Stadtwerke for allowing them to use and publish seismic and borehole data. Many thanks to M. Vernooij, P. Kuhn and S. Giger, whose input helped improving a first version of the manuscript. S. Muff is thanked for her help in finalising some of the figures in Petrosys®. This paper greatly benefited from the reviews of T. Diehl, D. Egli, A. G. Green and SJG editor S. M. Schmid.

References

Allen, P. A., Homewood, P., & Williams, G. D. (1986). Foreland basins: An introduction. *International Association of Sedimentologists, 8*, 3–12. **(Special Publication)**.

Allenbach, R. P., & Wetzel, A. (2006). Spatial patterns of Mesozoic facies relationships and the age of the Rhenish Lineament: A compilation. *International Journal of Earth Sciences, 95*, 803–813.

Bachmann, G. H., Dohr, G., & Müller, M. (1982). Exploration in a classic thrust belt and its foreland: Bavarian Alps, Germany. *American Association of Petroleum Geologists Bulletin, 66*, 2529–2542.

Berge, T. B., & Veal, S. L. (2005). Structure of the Alpine foreland. *Tectonics, 24*, TC5011.

Birkhäuser, P., Roth, P., Meier, B., & Naef, H. (2001). 3D-Seismik: Räumliche Erkundung der mesozoischen Sedimentschichten im Zürcher Weinland. *Nagra Technischer Bericht* (NTB 00-03). Wettingen: Nagra.

Breddin, H. (1964). Die tektonische Deformation der Fossilien und Gesteine in der Molasse von St. Gallen (Schweiz). *Geologische Mitteilungen, 4*, 1–68.

Burkhalter, R. M. (1996). Die Passwang-Alloformation (unteres Aalénien bis unteres Bajocien) im zentralen und nördlichen Schweizer Jura. *Eclogae Geologicae Helvetiae, 89*, 875–934.

Burkhard, M. (1990). Aspects of the large-scale Miocene deformation in the most external part of the Swiss Alps (Subalpine Molasse to Jura fold belt). *Eclogae Geologicae Helvetiae, 83*, 559–583.

Carlé, W. (1955). Über den Bau der Südwestdeutschen Grossscholle. *Zeitschrift der Deutschen Geologischen Gesellschaft, 103*, 60–67.

Chopra, S., & Marfurt, K. (2007). Seismic attributes for prospect identification and reservoir characterization. *SEG Geophysical Developments Series* 11 (464 pp.). USA: Society of Exploration Geophysicists Tulsa.

Conneally, J., Childs, C., & Walsh, J. (2014). Contrasting origins of breached relay zone geometries. *Journal of Structural Geology, 58*, 59–68.

Crampton, S. L., & Allen, P. A. (1995). Recognition of forebulge unconformities associated with early stage foreland basin development: Example from the North Alpine Foreland Basin. *American Association of Petroleum Geologists Bulletin, 79*, 1495–1514.

Deichmann, N. (1990). Seismizität der Nordschweiz 1987–1989 und Auswertung der Erdbebenserien von Günsberg, Läufelfingen und Zeglingen. *Nagra Technischer Bericht* (NTB 90-46). Wettingen: Nagra.

Deichmann, N., Ballarin Dolfin, D., & Kastrup, P. (2000). Seismizitat der Nord- und Zentralschweiz. *Nagra Technischer Bericht* (NTB 00-05). Wettingen: Nagra.

Diebold, P., Naef, H., & Ammann, M. (1991). Zur Tektonik der Zentralen Nordschweiz—Interpretation aufgrund regionaler Seismik, Oberflächengeologie und Tiefbohrungen. *Nagra Technischer Bericht* (NTB 90-41). Wettingen: Nagra.

Diehl, T., Clinton, J., Kraft, T., Husen, S., Plenkers, K., Guilhelm, A., et al. (2014a). Earthquakes in Switzerland and surrounding regions during 2013. *Swiss Journal of Geosciences, 107*, 359–375.

Diehl, T., Kraft, T., Kissling, E., Deichmann, N., Clinton, J., & Wiemer, S. (2014b). High-precision relocation of induced seismicity in the geothermal system below St. Gallen (Switzerland). *European Geophysical Union General Assembly 2014, Conference Abstracts*, *16*, 12541.

Edwards, B., Kraft, T., Cauzzi, C., Kästli, P., & Wiemer, S. (2015). Seismic monitoring and analysis of deep geothermal projects in St. Gallen and Basel. *Switzerland. Geophysical Journal International, 201*, 1022–1039.

Eugster, H., Fröhlicher, H., & Saxer, F. (1960). St. Gallen-Appenzell (map sheet 23), Explanatory Notes. *Geological atlas of Switzerland 1:25,000*. Bern: Schweizerische Geologische Kommission.

Fäh, D., Giardini, D., Kästli, P., Deichmann, N., Gisler, M., Schwarz-Zanetti, G., Alvarez-Rubio, S., Sellami, S., Edwards, B., Allmann, B., Bethmann, F., Wössner, J., Gassner-Stamm, G., Fritsche, S., & Eberhard, D. (2011). ECOS-09 Earthquake Catalogue of Switzerland Release 2011. *Report and database*. Public catalogue, 17.4.2011. Swiss Seismological Service, ETH Zürich. Report SED/RISK/R/001/20110417.

Gardner, G. H. F., Gardner, L. W., & Gregory, A. R. (1974). Formation velocity and density—the diagnostic basics for stratigraphic traps. *Geophysics, 39*, 770–780.

Habicht, K. (1945). Geologische Untersuchungen im südlichen sanktgallisch-appenzellischen Molassegebiet. *Beiträge zur Geologischen Karte der Schweiz* (166 pp.). Geologische Kommission der Schweizerischen Naturforschenden Gesellschaft.

Heidbach, O., & Reinecker, J. (2013). Analyse des rezenten Spannungsfelds der Nordschweiz. *Nagra Arbeitsbericht* (NAB 12-05). Wettingen: Nagra.

Hofmann, F. (1951). Zur Stratigraphie und Tektonik des st.gallisch-thurgauischen Miozäns (Obere Süsswassermolasse) und zur Bodenseegeologie. *Jahrbuch der St.Gallischen Naturwissenschaftlichen Gesellschaft*, *4*, 1–87.

Hofmann, F. (1973). Bischofszell (map sheet 1074). *Geological atlas of Switzerland 1:25,000*. Bern: Schweizerische Geologische Kommission.

Homewood, P., & Allen, P. (1981). Wave-, tide-, and current-controlled sandbodies of Miocene Molasse, Western Switzerland. *American Association of Petroleum Geologists Bulletin, 65*, 2534–2545.

Homewood, P., Allen, P. A., & Williams, G. D. (1986). Dynamics of the Molasse basin of western Switzerland. *Special Publications of the International Association of Sedimentologists, 8*, 199–217.

Kastrup, U., Zoback, M. L., Deichmann, N., Evans, K. F., Giardini, D., & Michael, A. J. (2004). Stress field variations in the Swiss Alps and the northern Alpine foreland derived from inversion of fault plane solutions. *Journal of Geophysical Research, 109*, B01402.

Kempf, O., Matter, A., Burbank, D. W., & Mange, M. (1999). Depositional and structural evolution of a foreland basin margin in a magnetostratigraphic framework: The eastern Swiss Molasse Basin. *International Journal of Earth Sciences, 88*, 253–275.

Leu, W. (2008). Permokarbon-Kartenskizze (Rohstoffe) Kompilation eines GIS-Datensatzes auf der Basis von bestehenden Unterlagen (Bereich Schweizer Mittelland). *Nagra Arbeitsbericht* (NAB 08-49). Wettingen: Nagra.

Madritsch, H. (2015). Outcrop-scale fracture systems in the Alpine foreland of central northern Switzerland: Kinematics and tectonic context. *Swiss Journal of Geosciences, 108*, 155–181.

Madritsch, H., Meier, B., Kuhn, P., Roth, P., Zingg, O., Heuberger, S., Naef, H., & Birkhäuser, P. (2013). Regionale strukturgeologische Zeitinterpretation der Nagra 2D-Seismik 2011/12. *Nagra Arbeitsbericht* (NAB 13-10). Wettingen: Nagra.

Mandl, G. (2000). *Faulting in brittle rocks: An introduction to the mechanics of tectonic faults* (434 pp.). Berlin: Springer.

Marchant, R., Ringgenberg, Y., Stampfli, G., Birkhäuser, P., Roth, P., & Meier, B. (2005). Paleotectonic evolution of the Zürcher Weinland (northern Switzerland), based on 2D and 3D seismic data. *Eclogae Geologicae Helvetiae, 98*, 345–362.

Marfurt, K. J., Sudhaker, V., Gersztenkorn, A., Crawford, K. D., & Nissen, S. E. (1999). Coherency calculations in the presence of structural dip. *Geophysics, 64*, 104–111.

Matter, A. (1987). Faciesanalyse und Ablagerungsmilieus des Permokarbons im Nordschweizer Trog. *Eclogae Geologicae Helvetiae, 80*, 345–367.

Matter, A., Homewood, P., Caron, C., Rigassi, D., van Stuijvenberg, J., Weidmann, M., & Winkler, W. (1980). Flysch and molasse of western and central Switzerland. In R. Trümpy (Ed.), *Geology of Switzerland, a guidebook (part B)* (pp. 261–292). Basel: Schweizerische Geologische Kommission, Wepf.

McCann, T., Pascal, C., Timmerman, M. J., Krzywiec, P., Lopez-Gomez, J., Wetzel, A., et al. (2006). Post-Variscan (end Carboniferous-Early Permian) basin evolution in Western and Central Europe. In D. G. Gee & R. A. Stephenson (Eds.), *European lithosphere dynamics* (pp. 355–388). Geological Society, London, Memoirs 32.

Meier, B., & Deplazes, G. (2014). Reflexionsseismische Analyse der Effinger Schichten. *Nagra Arbeitsbericht* (NAB 14-57). Wettingen: Nagra.

Müller, W. H., Naef, H., & Graf, H. R. (2002). Geologische Entwicklung der Nordschweiz, Neotektonik und Langzeitszenarien Zürcher Weinland. *Nagra Technischer Bericht* (NTB 99-08). Wettingen: Nagra.

Müller, M., Nieberding, F., & Wanninger, A. (1988). Tectonic style and pressure distribution at the northern margin of the Alps between Lake Constance and the River Inn. *Geologische Rundschau, 77*, 787–796.

Naef, H., Birkhäuser, P., & Roth, P. (1995). Interpretation der Reflexionsseismik im Gebiet nördlich Lägeren—Zürcher Weinland. *Nagra Technischer Bericht* (NTB 94-14). Wettingen: Nagra.

Naef, H., Diebold, P., & Schlanke, S. (1985). Sedimentation und Tektonik im Tertiär der Nordschweiz. *Nagra Technischer Bericht* (NTB 85-14). Wettingen: Nagra.

Naef, H., & Madritsch, H. (2014). Tektonische Karte des Nordschweizer Permokarbontrogs: Aktualisierung basierend auf 2D-Seismik und Schweredaten. *Nagra Arbeitsbericht* (NAB 14-17). Wettingen: Nagra.

Nagra (1989). Sondierbohrung Weiach—Untersuchungsbericht. *Nagra Technischer Bericht* (NTB 88-08). Wettingen: Nagra.

Nagra (2008). Vorschlag geologischer Standortgebiete für das SMA- und das HAA-Lager—Geologische Grundlagen. *Nagra Technischer Bericht* (NTB 08-04). Wettingen: Nagra.

Pavoni, N. (1980). Crustal stresses inferred from fault-plane solutions of earthquakes and neotectonic deformation in Switzerland. In A. E. Scheidegger (Ed.), *Tectonic stresses in the Alpine-Mediterranean region* (pp. 63–68). Vienna: Springer.

Pfiffner, O. A. (1986). Evolution of the north Alpine foreland basin in the Central Alps. *International Association of Sedimentologists, 8*, 219–228. **(Special Publication)**.

Pfiffner, O. A., Burkhard, M., Hänni, R., Kammer, A., Kligfield, R., Mancktelow, N. S., Menkveld, J. W., G., R. J., Schmid, S. M., & Zurbriggen, R. (2010). Structural Map of the Helvetic Zone of the Alps including Vorarlberg (Austria) and Haute Savoie (France). *Geological Special Map 128 (1:100,000)*. Federal Office of Topography Swisstopo, Wabern.

Pfiffner, O. A., Erard, P.-F., & Stäuble, M. (1997). Two cross sections through the Swiss Molasse basin (lines E4–E6, W1, W7–W10). In O. A. Pfiffner, P. Lehner, P. Heitzmann, S. Mueller, & A. Steck (Eds.), *Deep structure of the Swiss Alps: Results of NRP 20* (pp. 64–72). Basel: Birkhäuser.

Reicherter, K., Froitzheim, N., Jarosinski, M., Badura, J., Franzke, H.-J., Hansen, M., Hübscher, C., Müller, R., Poprawa, P., Reinecker, J., Stackebrandt, W., Voigt, T., von Eynatten, H., & Zuchiewicz, W. (2008). Alpine tectonics north of the Alps. In T. McCann (Ed.), *The geology of Central Europe* (pp. 1233–1285). Geological Society of London.

Reinecker, J., & Schneider, G. (2002). Zur Neotektonik der Zollernalb: Der Hohenzollerngraben und die Albstadt-Erdbeben. *Jahresberichte und Mitteilungen des oberrheinischen geologischen Vereins, 84*, 391–417.

Reinecker, J., Tingay, M., Müller, B., & Heidbach, O. (2010). Present-day stress orientation in the Molasse Basin. *Tectonophysics, 482*, 129–138.

Rotevatn, A., Tveranger, J., Howell, J. A., & Fossen, H. (2009). Dynamic investigation of the effect of a relay ramp on simulated fluid flow: Geocellular modelling of the Delicate Arch Ramp, Utah. *Petroleum Geoscience, 15*, 45–58.

Roth, P., Naef, H., & Schnellmann, M. (2010). Kompilation und Interpretation der Reflexionsseismik im Tafeljura und Molassebecken der Zentral- und Nordostschweiz. *Nagra Arbeitsbericht* (NAB 10-39). Wettingen: Nagra.

Rupf, I., & Nitsch, E. (2008). Das Geologisches Landesmodell von Baden-Württemberg: Datengrundlagen, technische Umsetzung und erste geologische Ergebnisse. *Landesamt für Geologie, Rohstoffe und Bergbau Baden-Würtemberg, Informationen* 21, 82 pp.

Saxer, F. (1964). Rorschach (map sheet 1075). *Geological atlas of Switzerland 1:25,000*. Bern: Schweizerische Geologische Kommission.

Schlunegger, F., Jordan, T. E., & Klaper, E. M. (1997). Controls of erosional denudation in the orogen on foreland basin evolution:

The Oligocene central Swiss Molasse Basin as an example. *Tectonics, 16*, 823–840.

Schlunegger, F., & Kissling, E. (2015). Slab rollback orogeny in the Alps and evolution of the Swiss Molasse basin. *Nature Communications, 6*, 1–10.

Schrader, F. (1988). Symmetry of pebble-deformation involving solution pits and slip-lineations in the northern Alpine Molasse Basin. *Journal of Structural Geology, 10*, 41–52.

Sinclair, H., & Allen, P. (1992). Vertical versus horizontal motions in the Alpine orogenic wedge: Stratigraphic response in the foreland basin. *Basin Research, 4*, 215–232.

Sommaruga, A. (2011). From the central Jura Mountains to the Molasse Basin (France and Switzerland). *Swiss Bulletin for Applied Geology, 16*, 63–75.

Sommaruga, A., Eichenberger, U., & Marillier, F. (2012). Seismic Atlas of the Swiss Molasse Basin. Edited by the Swiss Geophysical Commission. *Matériaux pour la Géologie de la Suisse—Géophysique,* 44.

Sprecher, C., & Müller, W. H. (1986). Geophysikalisches Untersuchungsprogramm Nordschweiz: Relexionsseismik 82. *Nagra Technischer Bericht* (NTB 84-15). Wettingen: Nagra.

Swisstopo, (2005). *Tektonische Karte der Schweiz 1:500,000*. Wabern: Federal Office of Topography Swisstopo.

Volz, E. (1957). *Geologische Ergebnisse neuerer Erdölbohrungen in Oberschwaben*, PhD Thesis, Technische Hochschule Stuttgart, 71 pp.

Walsh, J. J., Watterson, J., Bailey, W. R., & Childs, C. (1999). Fault relays, bends and branch lines. *Journal of Structural Geology, 21*, 1019–1026.

Wetzel, A., Allenbach, R., & Allia, V. (2003). Reactivated basement structures affecting the sedimentary facies in a tectonically "quiescent" epicontinental basin: An example from NW Switzerland. *Sedimentary Geology, 157*, 153–172.

Wiemer, S., Giardini, D., Fäh, D., Deichmann, N., & Sellami, S. (2009). Probabilistic seismic hazard assessment of Switzerland: Best estimates and uncertainties. *Journal of Seismology, 13*, 449–478.

Withjack, M. O., Olson, J., & Peterson, E. (1990). Experimental models of extensional forced folds. *American Association of Petroleum Geologists Bulletin, 74*, 1038–1054.

Ziegler, P. A. (1990). *Geological atlas of Western and Central Europe* (2nd ed.). Shell International Petroleum Maatschappij B.V., distributed by Geological Society London, 239 pp.

Ziegler, P. A., & Dèzes, P. (2006). Crustal evolution of Western and Central Europe. In D. G. Gee & R. A. Stephenson (Eds.), *European lithosphere dynamics* (pp. 43–56). Geological Society, London, Memoirs 32.

Ziegler, P. A., & Dèzes, P. (2007). Cenozoic uplift of Variscan Massifs in the Alpine foreland: Timing and controlling mechanisms. *Global and Planetary Change, 58*, 237–269.